On the quark mass dependence of exotic resonances

R. Molina (Raquel.Molina@ific.uv.es)

Zejian Zhuang, Fernando Gil, Alessandro Giachino, Lisheng Geng, Junxu Lu

August 18, 2025

Content

Godfrey-Isgur Quark Model

PHYSICAL REVIEW D VOLUME 32, NUMBER 1 1 JULY 1985

Mesons in a relativized quark model with chromodynamics

Stephen Godfrey and Nathan Isgur
Department of Physics, University of Toronto, Toronto, M5S 1A7 Canada
(Received 12 December 1983; revised manuscript received 10 May 1985)

We show that mesons—from the π to the Υ—can be described in a unified quark model with chromodynamics. The key ingredient of the model is a universal one-gluon-exchange-plus-linear-confinement potential motivated by QCD, but it is crucial to the success of the description to take into account relativistic effects. The spectroscopic results of the model are supported by an extensive analysis of strong, electromagnetic, and weak meson couplings.

$$H\,|\,\Psi\rangle=(H_0+V)\,|\,\Psi\rangle=E\,|\,\Psi\rangle$$

$$H_0\rightarrow\sum_{i=1}^{2}\left[m_i+\frac{p^2}{2m_i}\right] \tag{2a}$$

and

$$V_{ij}(\mathbf{p},\mathbf{r})\rightarrow H_{ij}^{\rm conf}+H_{ij}^{\rm hyp}+H_{ij}^{\rm so}+H_A \tag{2b}$$

where

$$H_{ij}^{\rm conf}=-\left[\tfrac{3}{4}c+\tfrac{3}{4}br-\frac{\alpha_s(r)}{r}\right]\mathbf{F}_i\cdot\mathbf{F}_j \tag{3}$$

includes the spin-independent linear confinement and Coulomb-type interactions,

$$H_{ij}^{\rm hyp}=-\frac{\alpha_s(r)}{m_i m_j}\left[\frac{8\pi}{3}\mathbf{S}_i\cdot\mathbf{S}_j\delta^3(\mathbf{r})+\frac{1}{r^3}\left[\frac{3\mathbf{S}_i\cdot\mathbf{r}\mathbf{S}_j\cdot\mathbf{r}}{r^2}-\mathbf{S}_i\cdot\mathbf{S}_j\right]\right]\mathbf{F}_i\cdot\mathbf{F}_j$$

is the color hyperfine interaction, and

$$H_{ij}^{\rm so}=H_{ij}^{\rm so(cm)}+H_{ij}^{\rm so(tp)} \tag{5}$$

is the spin-orbit interaction with

$$H_{ij}^{\rm so(cm)}=-\frac{\alpha_s(r)}{r^3}\left[\frac{1}{m_i}+\frac{1}{m_j}\right]\left[\frac{\mathbf{S}_i}{m_i}+\frac{\mathbf{S}_j}{m_j}\right]\cdot\mathbf{L}\,(\mathbf{F}_i\cdot\mathbf{F}_j)\,, \tag{6}$$

its color-magnetic piece and with

$$H_{ij}^{\rm so(tp)}=\frac{-1}{2r}\frac{\partial H_{ij}^{\rm conf}}{\partial r}\left[\frac{\mathbf{S}_i}{m_i{}^2}+\frac{\mathbf{S}_j}{m_j{}^2}\right]\cdot\mathbf{L} \tag{7}$$

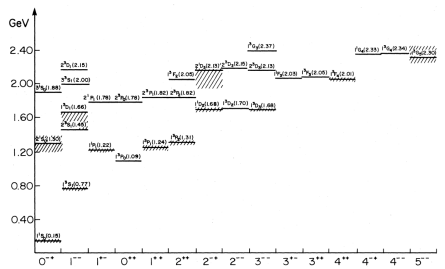

Godfrey-Isgur Quark Model

- Difficulties to explain the masses of some excited states ...
- In particular the **scalar mesons** $J^{PC} = 0^{++}$, σ, κ, $f_0(980)$, $a_0(980)$, which decay in two pseudoscalar mesons, $\pi\pi/\pi K/K\bar{K}$

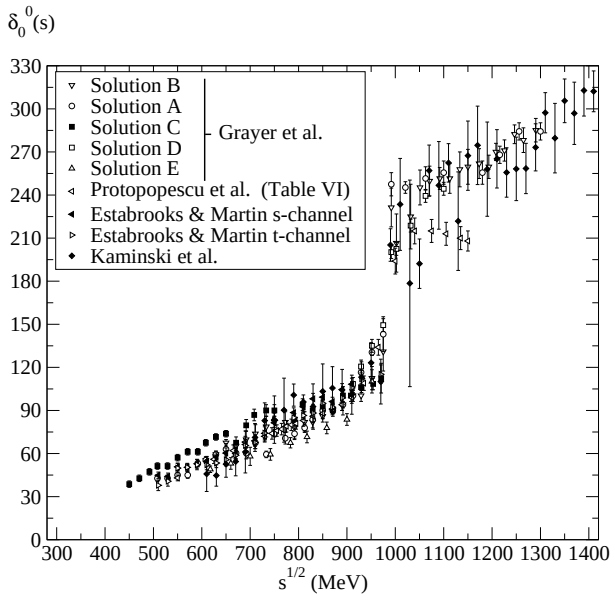

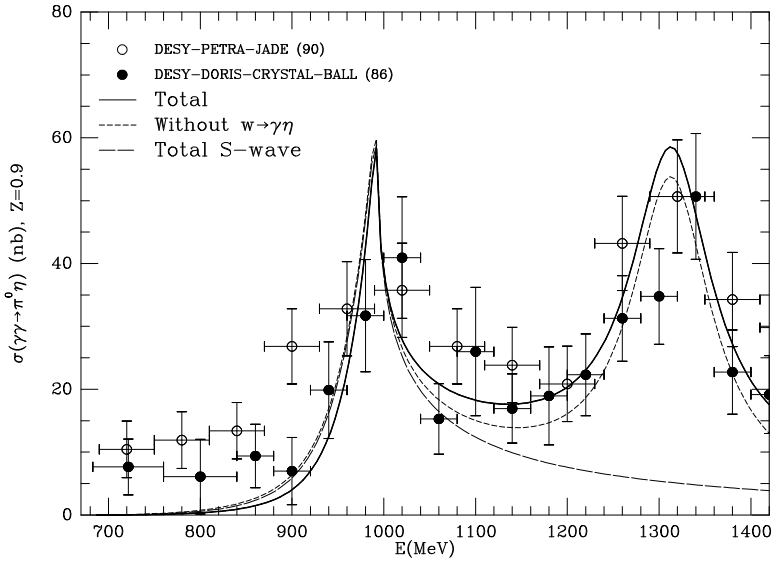

- Other mesons difficult to explain: $f_0(1500)$, $f_0(1370)$, $J^{PC} = 0^{++}$
- Mesons observed with quantum numbers that **cannot be obtained with** $q\bar{q}$, $\pi_1(1400)$, $\pi_1(1600)$, $J^{PC} = 1^{-+}$ ...
- Other examples in the baryon sector: $N(1440)$, $\Lambda(1405)$ ...

Hadrons

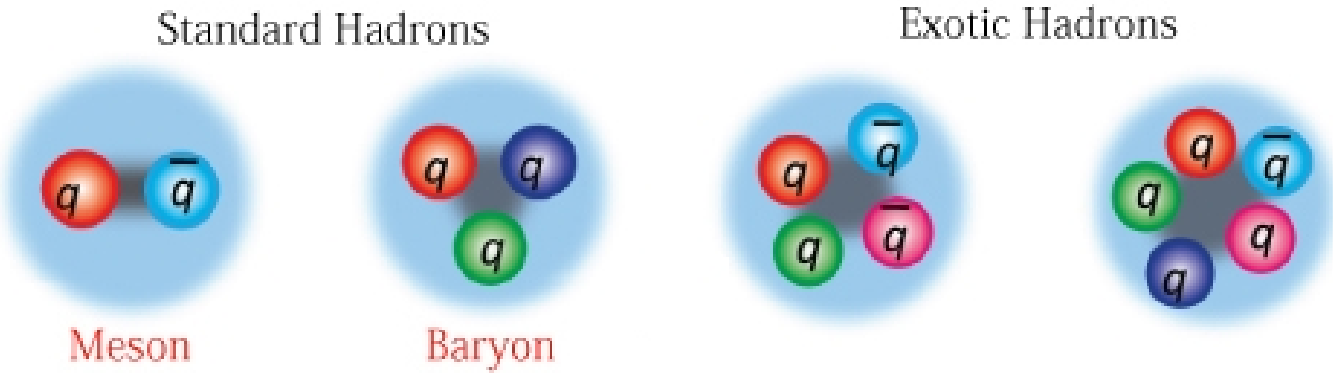

- 'Regular' hadrons: $q\bar{q}$, qqq

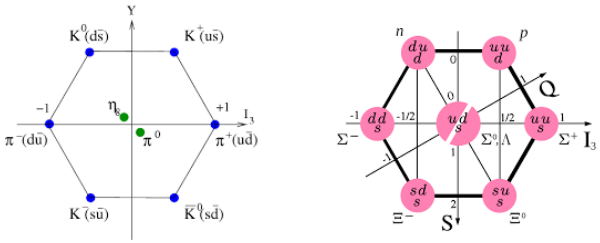

- Exotics: $q\bar{q}q\bar{q}$, $qqqq\bar{q}$, qqg,...
  Not $q\bar{q}$: $J^{PC} = 0^{+-}, 1^{-+}, 2^{+-}, 3^{-+}$,...

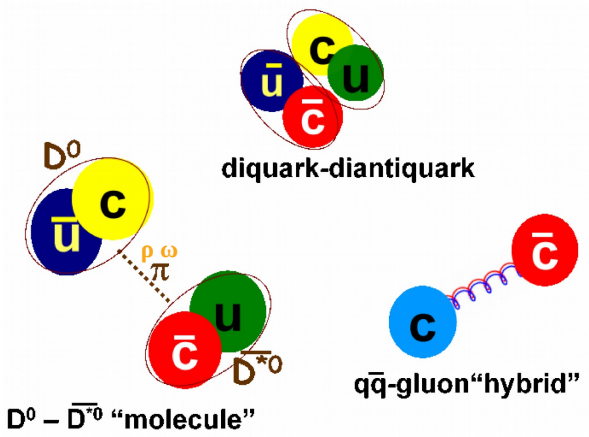

Exotics: The X(3872)

PRL03, BELLE (close to $D^0 \bar{D}^{*0}$ th.)

ABSTRACT

We report the observation of a narrow charmoniumlike state produced in the exclusive decay process $B^{\pm} \to K^{\pm}\pi^{+}\pi^{-}J/\psi$. This state, which decays into $\pi^{+}\pi^{-}J/\psi$, has a mass of $3872.0 \pm 0.6(\mathrm{stat}) \pm 0.5(\mathrm{syst})$ MeV, a value that is very near the $M_{D^0} + M_{D^{*0}}$ mass threshold. The results are based on an analysis of 152M B-$\overline{B}$ events collected at the $\Upsilon(4S)$ resonance in the Belle detector at the KEKB collider. The signal has a statistical significance that is in excess of 10σ.

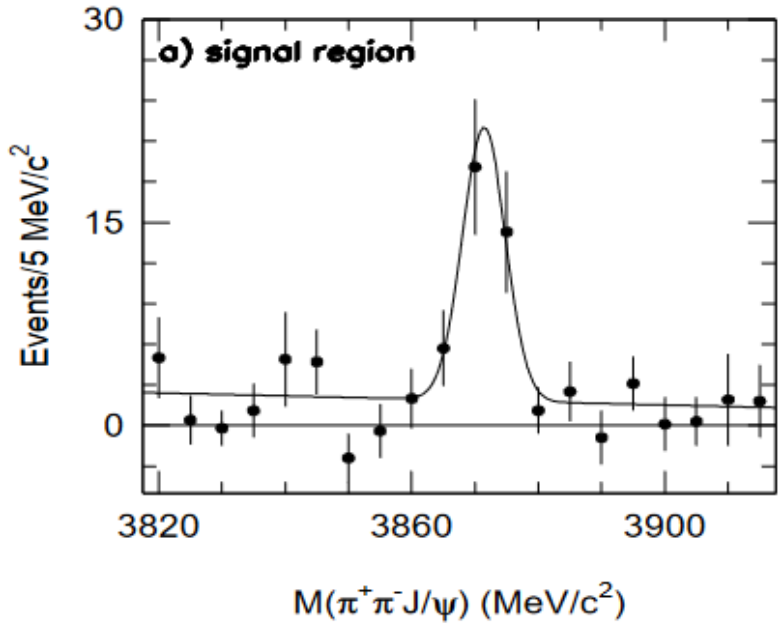

Tornqvist, ClosePage, Voloshin04, Braaten05, Swanson06, Gamermann0set07

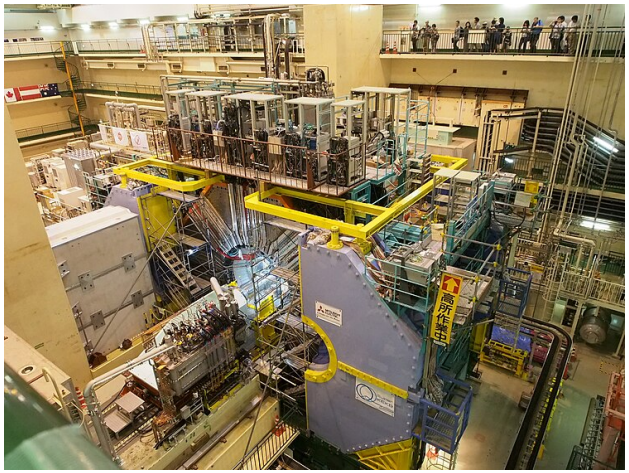

The measured mass of the state is within errors of the $D^0\bar{D}^{*0}$ mass threshold (3871.3 ± 0.5 MeV [7]). This would be expected for a loosely bound $D\bar{D}^*$ multiquark "molecular state," such as proposed by De Rujula, Georgi and Glashow in 1977 [13].

CONCLUSION

We have observed a strong signal (8.6σ) for a state that decays to $\pi^{+}\pi^{-}J/\psi$ with

$$M = 3871.8 \pm 0.7\ (\mathrm{stat}) \pm 0.4\ (\mathrm{syst})\ \mathrm{MeV}$$
$$\Gamma < 3.5\ \mathrm{MeV}\ .$$

This mass value is about 60 MeV higher than potential model predictions for a 1D charmonium state and equal, within errors, to $M_{D^0} + M_{D^{*0}}$. This coincidence with the $D^0\bar{D}^{*0}$ mass threshold suggests that this may be a DD^* multiquark state.

$$m_X - m_{D^{*0}} - m_{\bar{D}^0} = 1.1 \pm 0.7\ \mathrm{MeV};\ \Gamma_X = 1.19 \pm 0.21$$

$$\mathrm{MeV\ PDG25};\ \Gamma(X \to D^{*0}\bar{D}^0) \sim \frac{p_{D^*}\, g^2_{XD^{*0}\bar{D}^0}}{8\pi M_X^2}$$

Evidence on LQCD Prelovsek13 PRL ($\Delta E = 11 \pm 7$ MeV)

Exotics: The $D_{s0}(2317)$ and $D_{s1}(2460)$

BABAR, CLEO'03

PHYSICAL REVIEW LETTERS

Highlights Recent Accepted Collections Authors Referees Search Press Ab

Observation of a Narrow Meson State Decaying to $D_s^+\pi^0$ at a Mass of $2.32\ \mathrm{GeV}/c^2$

B. Aubert *et al.* (BABAR Collaboration)
Phys. Rev. Lett. **90**, 242001 – Published 17 June 2003

- Babar observed
  $D_{s0}^{*+}(2317) \to D_s^+ \pi^o$
  Phys. Rev. Lett. 90(2003)242001
- Cleo observed
  $D_{s1}^+(2460) \to D_s^{+*} \pi^o$
  Phys. Rev. D 68(2003)032002
- D_s in final state
  > most probable assignment
  $[c\ \bar{s}]$ L=1 states
- ~100 MeV too low compared to early quark models
  Godfrey, Isgur, PRD 32(1985)189

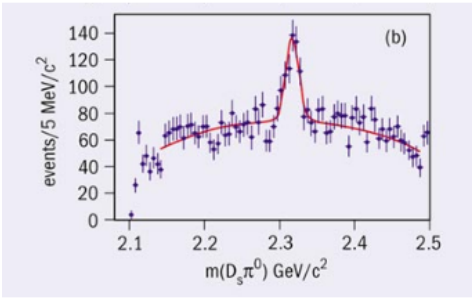

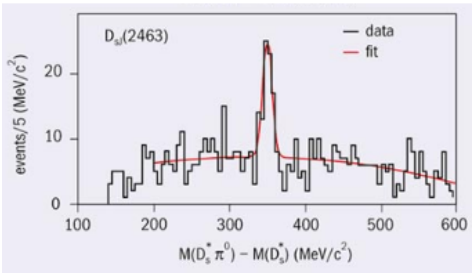

Similar masses to the DK, DK^* thresholds
Liu, Orginos, F. K. Guo, Meissner, PRD13
F. K. Guo et al. RMP18

$T_{cc}^{+}(3875)$ signal in $D^0 D^0 \pi^+$ LHCb, Nature (2022)

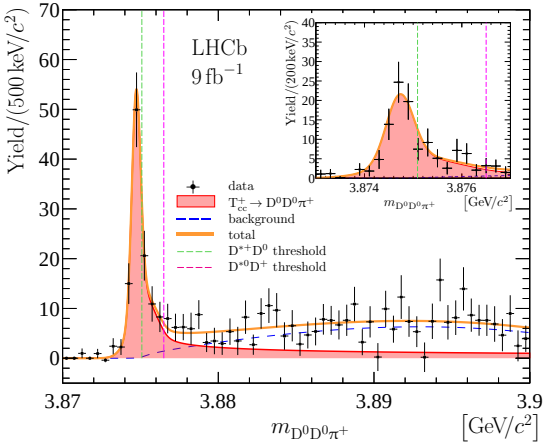

BEFORE resolution:

$$m_{\text{exp}} = 3875.09 \text{ MeV} + \delta m_{\text{exp}}$$

$$\delta m_{\text{exp}} = -273 \pm 61 \pm 5^{+11}_{-14} \text{ keV};$$

$$\Gamma = 410 \pm 165 \pm 43^{+18}_{-38} \text{ keV}$$

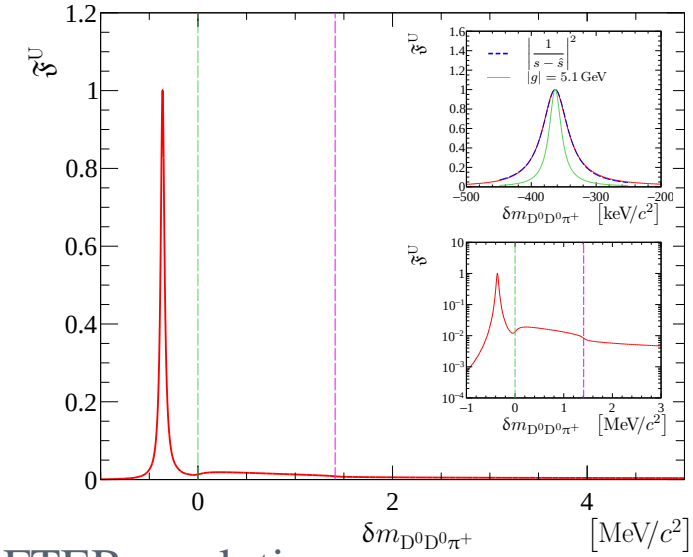

AFTER resolution

$$\delta m_{\text{exp}} = -360 \pm 40^{+4}_{-0} \text{ keV};$$

$$\Gamma = 48 \pm 2^{+0}_{-14} \text{ keV}$$

Feijoo, Liang, Oset, PRD21 (HGF)

Close to the $D^{*+}D^0/D^{*0}D^+$!!

$$\frac{d\Gamma}{dM_{12}^2\, dM_{23}^2} = \frac{1}{2}\,\frac{1}{(2\pi)^3}\,\frac{1}{s^{3/2}}\,|t|^2, \Longrightarrow \Gamma = 43 \text{ KeV}$$

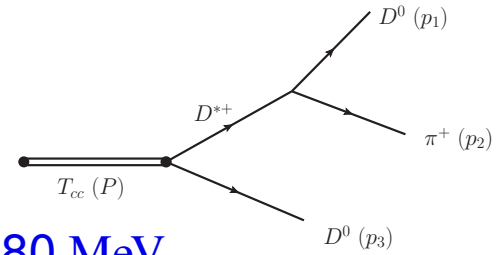

LQCD, Padmanath, Prelovsek, PRL22, $\Delta E \simeq 9.9$ MeV, 280 MeV

Quark mass dependence of the $D(D^*)$ mesons

Heavy Hadron Chiral Perturbation Theory (HHχPT)

E. Jenkins, NPB412 (1994); Gil-Domínguez, Molina PLB (2023)

$$\frac{1}{4}(D+3D^*) = m_H + \alpha_a - \sum_{X=\pi,K,\eta} \beta_a^{(X)} \frac{M_X^3}{16\pi f^2} + \sum_{X=\pi,K,\eta} \left(\gamma_a^{(X)} - \lambda_a^{(X)}\alpha_a\right) \frac{M_X^2}{16\pi^2 f^2} \log\left(M_X^2/\mu^2\right) + c_a$$

$$(D^* - D) = \Delta + \sum_{X=\pi,K,\eta} \left(\gamma_a^{(X)} - \lambda_a^{(X)}\Delta\right) \frac{M_X^2}{16\pi^2 f^2} \log\left(M_X^2/\mu^2\right) + \delta c_a$$

$\mu = 770$ MeV; $g^2 = 0.55$ MeV (Decay of the D^* meson)

$$\left.\begin{aligned} \frac{1}{4}(D+3D^*) &= m_H + f(\sigma, a, b, c, d) \\ (D^* - D) &= \Delta + g(\Delta^{(\sigma)}, \Delta^{(a)}) \end{aligned}\right\}$$

9 parameters, but different collaborations/scale settings, $7 + 2 \times 7 = 21$ parameters, ~ 80 data points

ETMC, PACS, HSC, CLS, RQCD, S.Prelovsek, MILC

$D(D^*)$ quark mass dependence

LASSO + information criteria;

$$\chi^2_P = \chi^2 + \lambda \sum_i^n |p_i|; \quad \text{Data} = \text{Training (70\%)} + \text{Test (30\%)} \qquad (1)$$

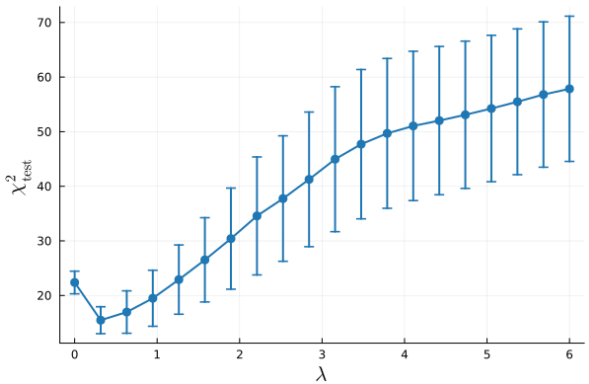

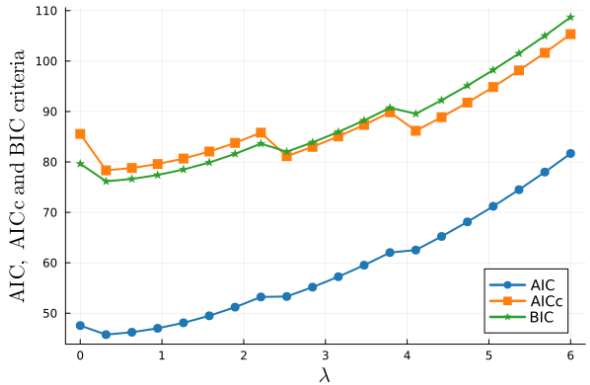

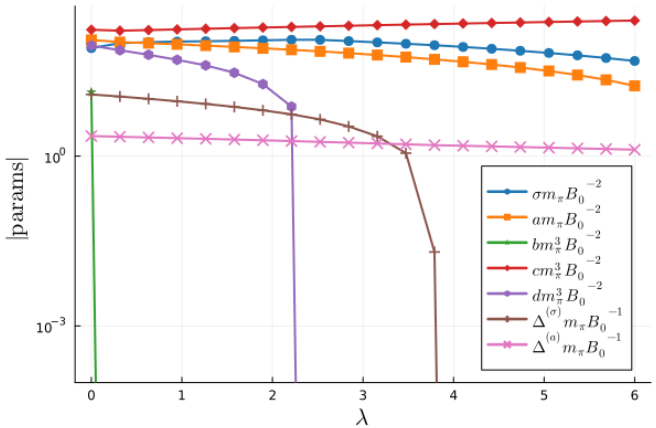

Some of the parameters are not relevant
Plots for ETMC data analysis

$D(D^*)$ quark mass dependence

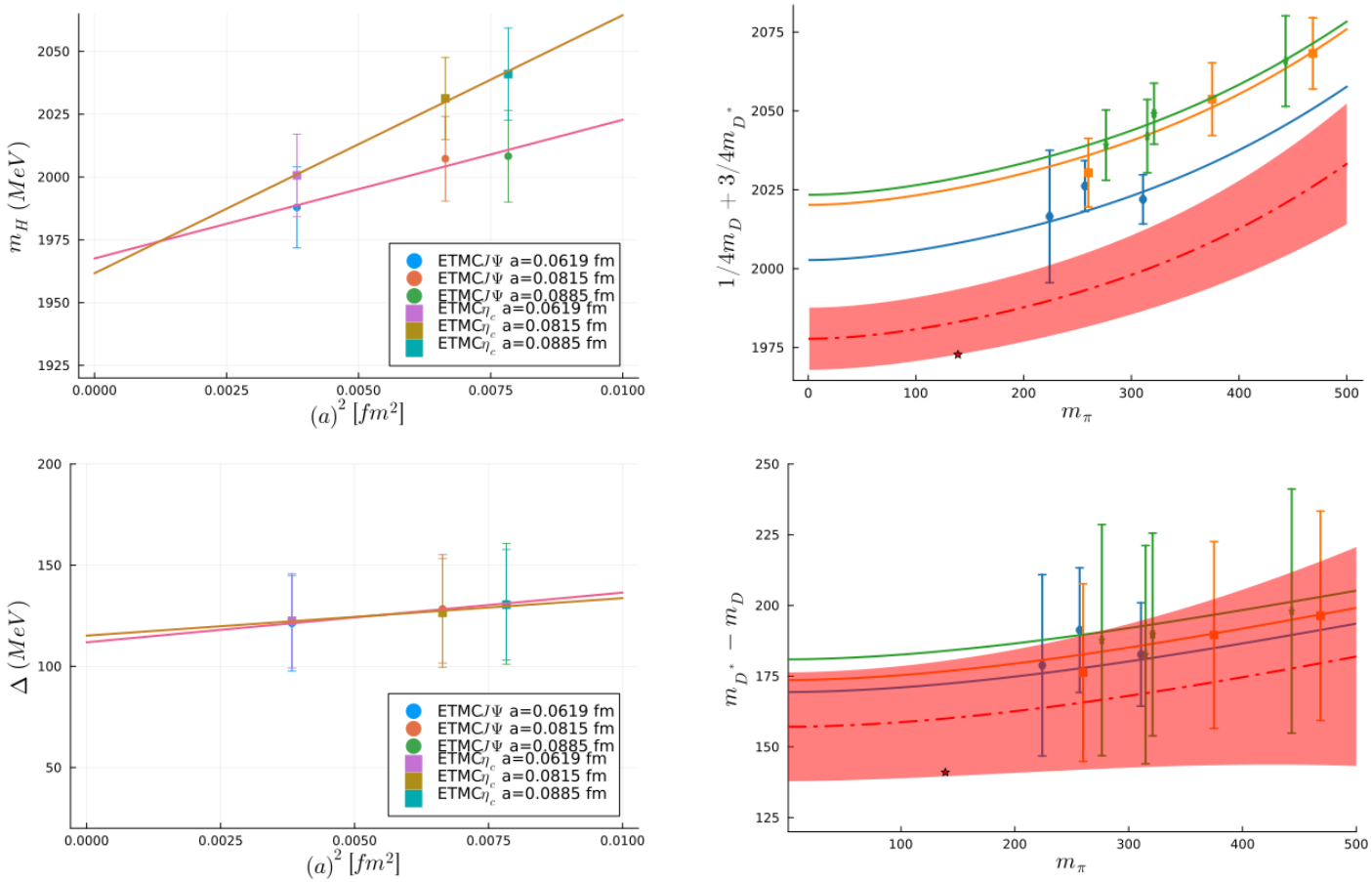

Figure: Extrapolation to the physical point of the ETMC data. $m_H = m'_H + r_H a^2$, $\Delta = \Delta' + r_\Delta a^2$.

Global analysis

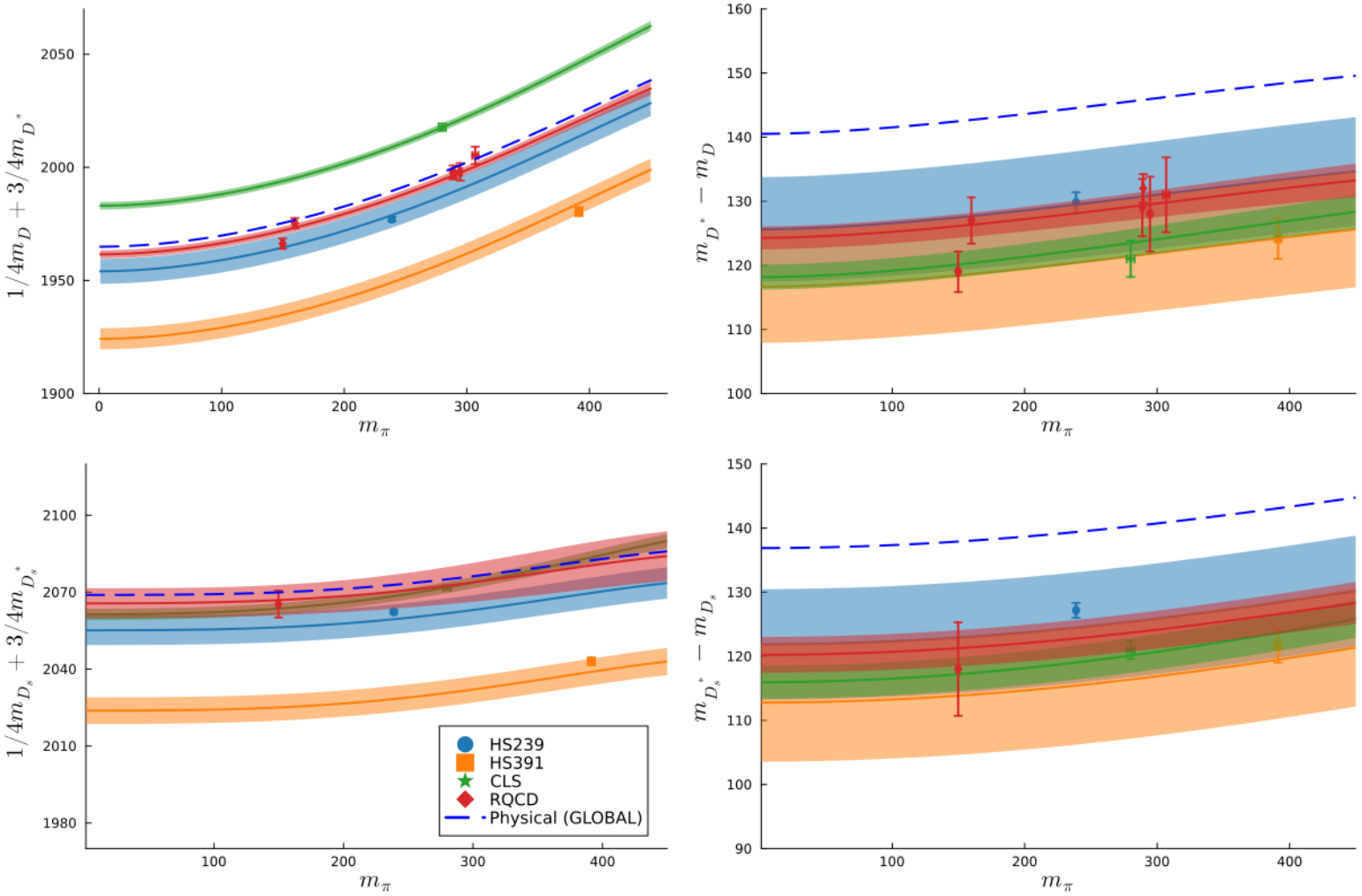

Figure: Results of the D, D^*, D_s and D_s^* meson masses for the global analysis of some collaborations.

Results for the T_{cc}

Lagrangian HGF Bando, Kugo, Yamawaki, PRL54

$$\mathcal{L} = \mathcal{L}^{(2)} + \mathcal{L}_{III} \tag{2}$$

$$\mathcal{L}^{(2)} = \frac{1}{4} f^2 \langle D_\mu U D^\mu U^\dagger + \chi U^\dagger + \chi^\dagger U \rangle, \quad \mathcal{L}_{III} = -\frac{1}{4} \langle V_{\mu\nu} V^{\mu\nu} \rangle + \frac{1}{2} M_V^2 \langle [V_\mu - \frac{i}{g} \Gamma_\mu]^2 \rangle$$

Some of the vertices: $\mathcal{L}_{V\gamma} = -M_V^2 \frac{e}{g} A_\mu \langle V^\mu Q \rangle$, $g = \frac{M_V}{2f}$

$\mathcal{L}_{VPP} = -ig \langle V^\mu [P, \partial_\mu P] \rangle$, $\mathcal{L}_{III}^{(3V)} = ig \langle (\partial_\mu V_\nu - \partial_\nu V_\mu) V^\mu V^\nu \rangle$, ...

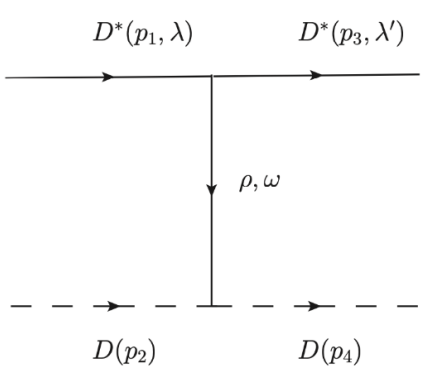

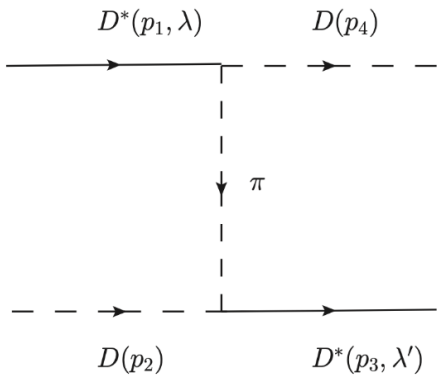

$$V_\mu = \begin{pmatrix} \frac{\rho^0}{\sqrt{2}} + \frac{\omega}{\sqrt{2}} & \rho^+ & K^{*+} & \bar{D}^{*0} \\ \rho^- & -\frac{\rho^0}{\sqrt{2}} + \frac{\omega}{\sqrt{2}} & K^{*0} & D^{*-} \\ K^{*-} & \bar{K}^{*0} & \phi & D_s^{*-} \\ D^{*0} & D^{*+} & D_s^{*+} & J/\psi \end{pmatrix}_\mu$$

Results for the T_{cc}

(including only vector meson exchange)

$$V^{\rho(I=0)}_{\lambda,\lambda'}(p,p') = -g^2 \frac{(p_1+p_3)_\mu (p_2+p_4)^\mu}{t-m_\rho^2} \epsilon_{\lambda,\nu}(p_1)\epsilon^{*}_{\lambda'}{}^{\nu}(p_3) \qquad (3)$$

and $g = g_1 + g_2\, m_\pi^2$. Quark mass dependence of m_ρ, Molina, Elvira, JHEP20

Col.	a	L	m_π
Padmanath22,Collins24	0.086	2 – 3	280
HSC24	0.120	1.9 – 2.9	391
CLQCD Chen22	0.152	2.4	349

Col.	a	m_π	a_0^{-1}
HALQCD23	0.0846	146	0.05
HALQCD14	0.0907	411	2.34

Infinite Volume

Scattering amplitude (Bethe-Salpeter):

$$T^{-1} = V_0^{-1} - G\,. \tag{4}$$

where $V_0 \equiv V_{(L=0)}$ is the s-wave projection.

$$G_j = i \int \frac{d^4q}{(2\pi)^4} \frac{1}{q^2 - m_j^2 + i\epsilon} \frac{1}{(P-q)^2 - M_j^2 + i\epsilon}\,. \tag{5}$$

The loop function can be evaluated in the Dimensional Regularization (DR) or cutoff scheme ($q_{\max}$). Oller, Meissner, PLB01:

$$G_i(s) = \frac{1}{16\pi^2}\left\{ a_i(\mu) + \ln\frac{M_i^2}{\mu^2} + \frac{m_i^2 - M_i^2 + s}{2W^2}\ln\frac{m_i^2}{M_i^2} \right.$$

$$+\frac{\bar{q}_i}{\sqrt{s}}\left[\ln(\ s - (M_i^2 - m_i^2) + 2\bar{q}_i\sqrt{s}) + \ln(\ s + (M_i^2 - m_i^2) + 2\bar{q}_i\sqrt{s})\right.$$

$$\left.\left. - \ln(-s + (M_i^2 - m_i^2) + 2\bar{q}_i\sqrt{s}) - \ln(-s - (M_i^2 - m_i^2) + 2\bar{q}_i\sqrt{s})\right]\right\},$$

Infinite Volume

Oller, PPNP20:

$$a(\mu) = -\frac{2}{m_i + M_i}\left[m_i \log(1 + \sqrt{1 + \frac{m_i^2}{q_{\max}^2}}) + M_i \log(1 + \sqrt{1 + \frac{M_i^2}{q_{\max}^2}})\right] + 2\log(\frac{\mu}{q_{\max}}). \quad (6)$$

with $\mu = 630$ MeV (Oset, Ramos, NPA98). Analytical continuation of G:

$$G_i^{II}(s) = G_i(s) + i\,\frac{q_{\rm cm}}{4\pi\sqrt{s}}, \qquad {\rm Im}q_{\rm cm} > 0. \quad (7)$$

Near to the resonance region:

$$T_{ij} \simeq \frac{g_i g_j}{s - s_0}, \quad (8)$$

g_i coupling to the channel i. The phase shift is:

$$p\cot\delta_j = -8\pi E (T_{jj})^{-1} + i\,p_j\,, \quad (9)$$

Finite volume

Finite volume scattering amplitude:

$$\tilde{T}^{-1} = V_0^{-1} - \tilde{G}\,, \tag{10}$$

Loop function $\tilde{G}$ (DR),

$$\widetilde{G}(P^0, \vec{P}) = G^{DR}(P^0, \vec{P}) + \lim_{q_{\max}\to\infty} \Delta G(P_0, \vec{P}, q_{\max}), \tag{11}$$

G^{DR}: loop function in the infinite volume, $\Delta G = \tilde{G}^{co} - G^{co}$.
Loop function (cutoff):

$$\tilde{G}^{co} = \frac{1}{L^3} \sum_n^{q_{\max}} \frac{E}{P_0} I(q^*)\,, \tag{12}$$

q^*: center-of-mass (CM) momentum, $\vec{q}_1{}^* + \vec{q}_2{}^* = 0$, $P^\mu = q_1^\mu + q_2^\mu$,
$s = P_0^2 - \vec{P}^{\,2}$.

Finite volume

The function $I(q)$ reads,

$$I(\vec{q}) = \frac{\omega_1(q) + \omega_2(q)}{2\omega_1(q)\omega_2(q)\left[P_0^2 - (\omega_1(q) + \omega_2(q))^2 + i\epsilon\right]}, \tag{13}$$

with $\omega_i = \sqrt{q^2 + m_i^2}$, and $q = |\vec{q}\,|$.

The energy levels are given by,

$$\det(\delta_{ll'}\delta_{mm'} - V_l \tilde{G}_{lm,l'm'}) = 0\,. \tag{14}$$

We take into account the covariance matrix of the energy levels from the LQCD simulation.

$$\chi^2 = \Delta E^T C_E^{-1} \Delta E \tag{15}$$

$q_{\max} = 612 \pm 29$ MeV, $g_0 = 3.13 \pm 0.10$, $g_2 m^2_{\text{phys}} = -0.057 \pm 0.058$

Results for the T_{cc}

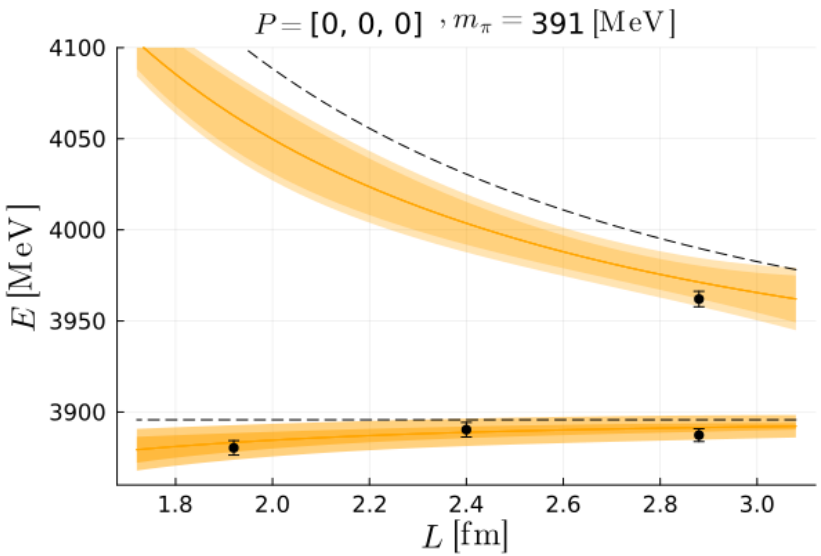

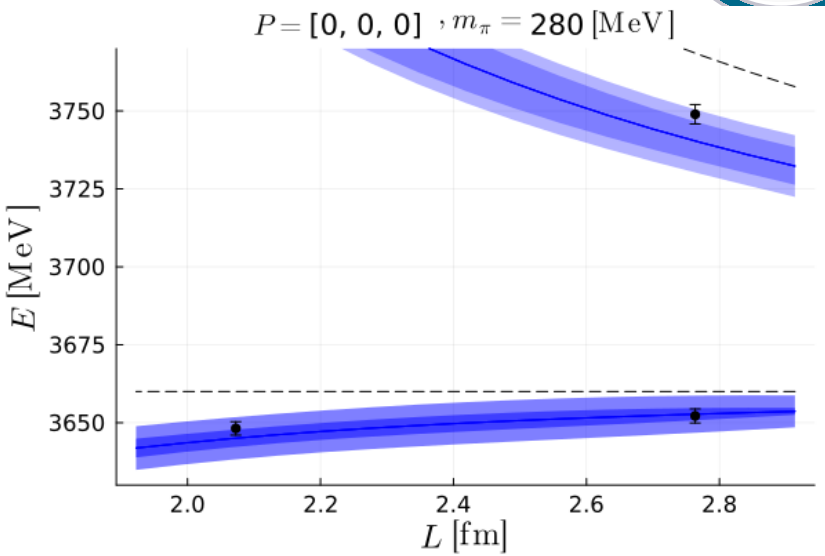

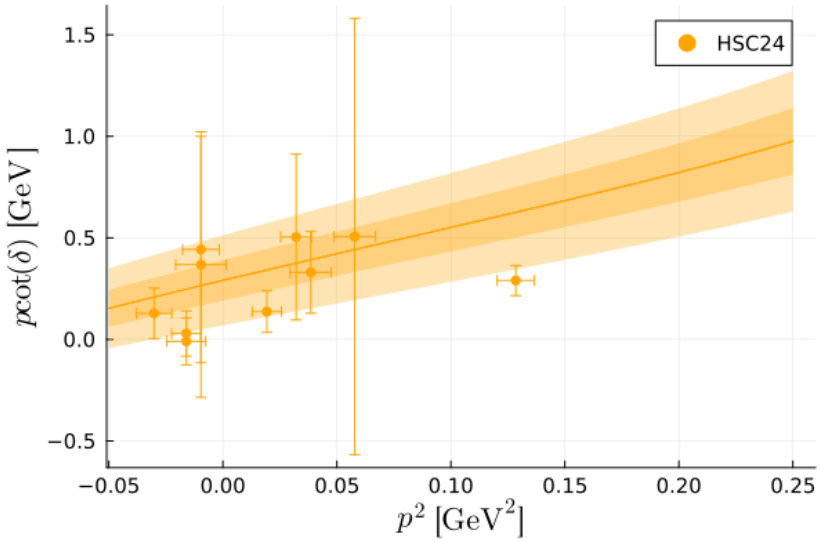

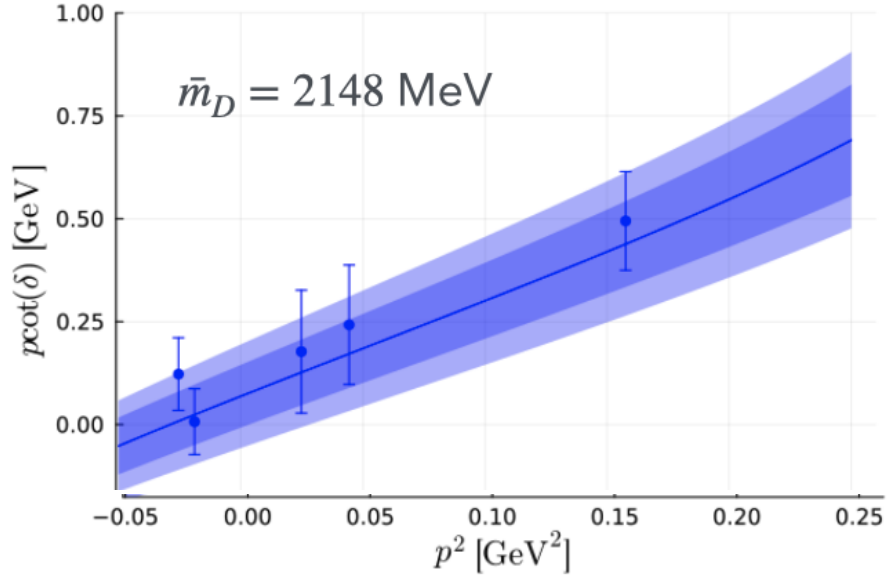

Results for the T_{cc}

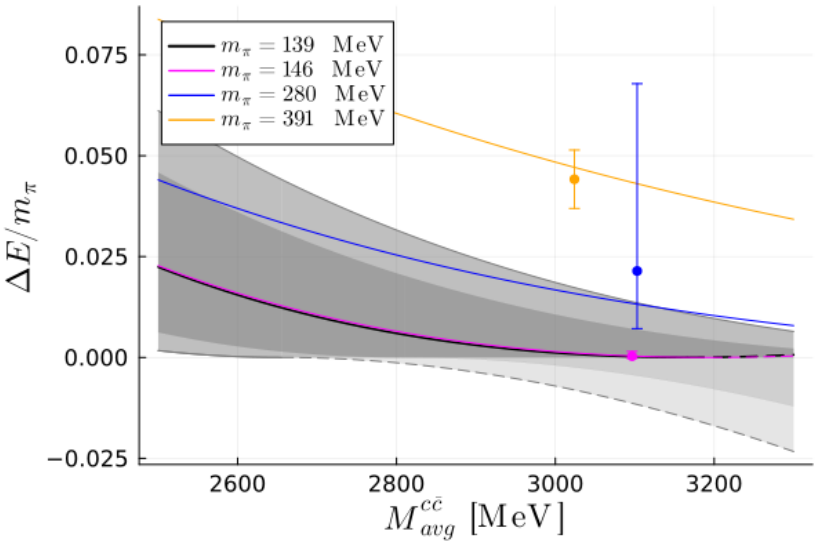

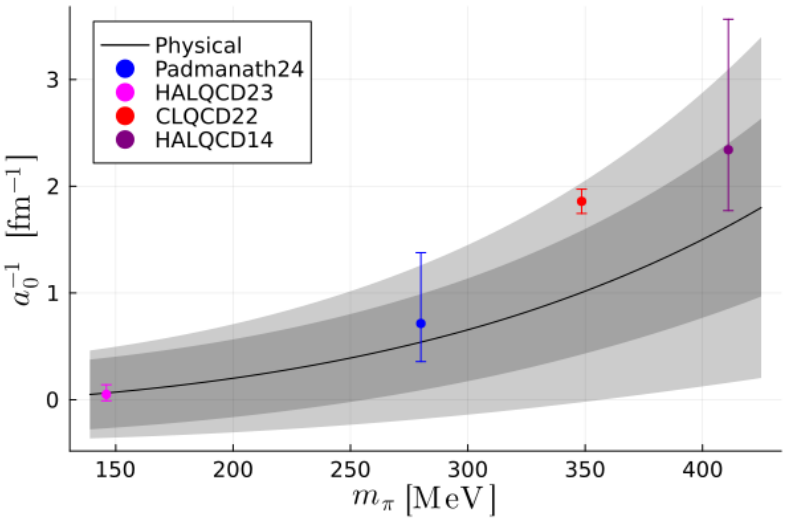

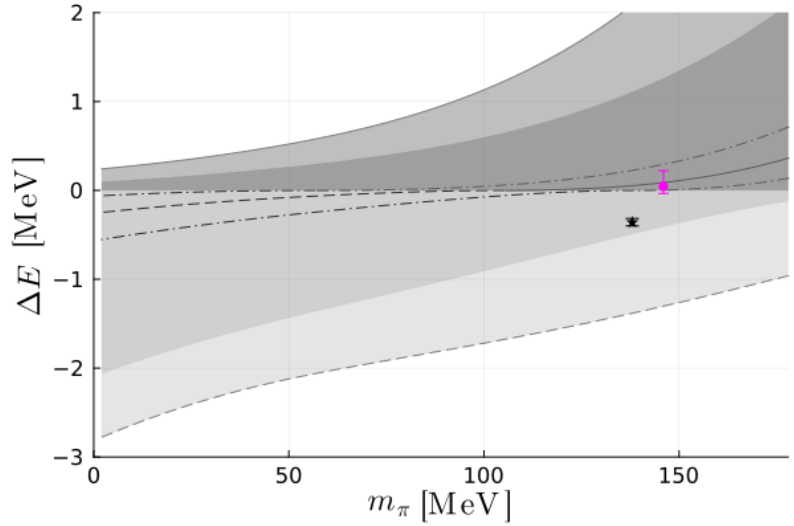

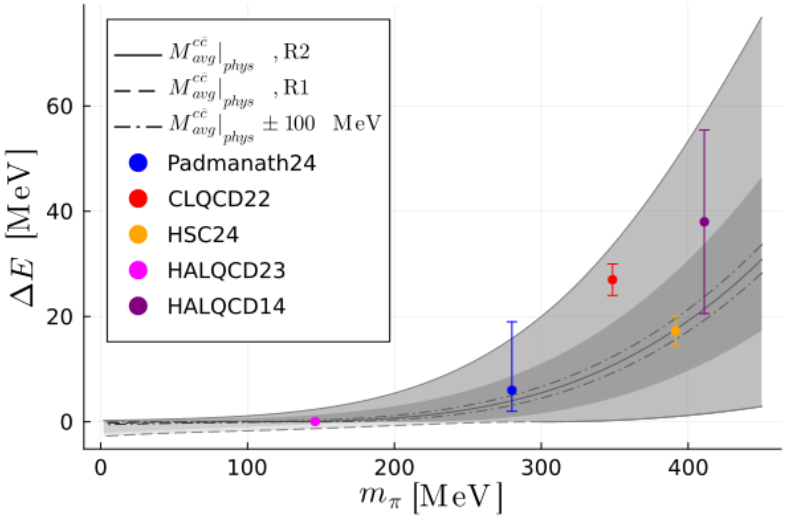

Results for the T_{cc}

Momentum dependent BS equation including $\pi + \rho$, finite width D^*

$$V^{\pi(I=0)}_{\lambda,\lambda'}(p,p') = \frac{3}{4} g^2_{D^* D\pi} \frac{e^{u/\Lambda^2}}{u - m^2_\pi} (2p_4 - p_1)_\mu \epsilon^\mu_\lambda(p_1) \, (2p_2 - p_3)_\nu \epsilon^{*,\nu}_{\lambda'}(p_3)$$

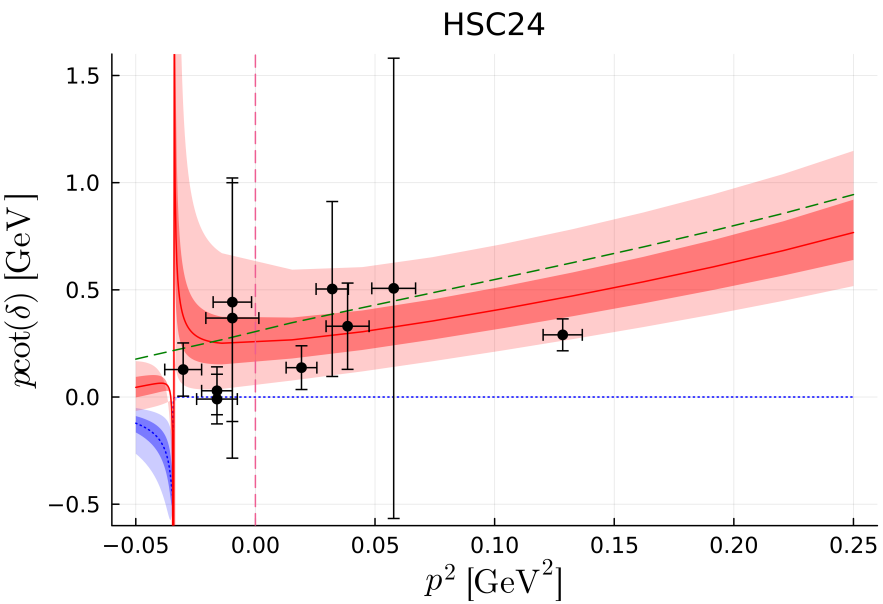

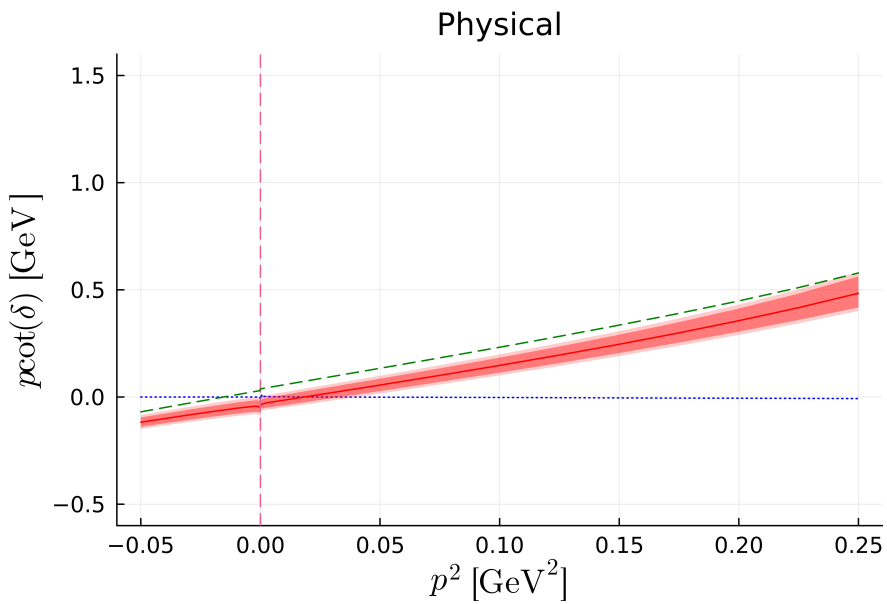

Results for the T_{cc}

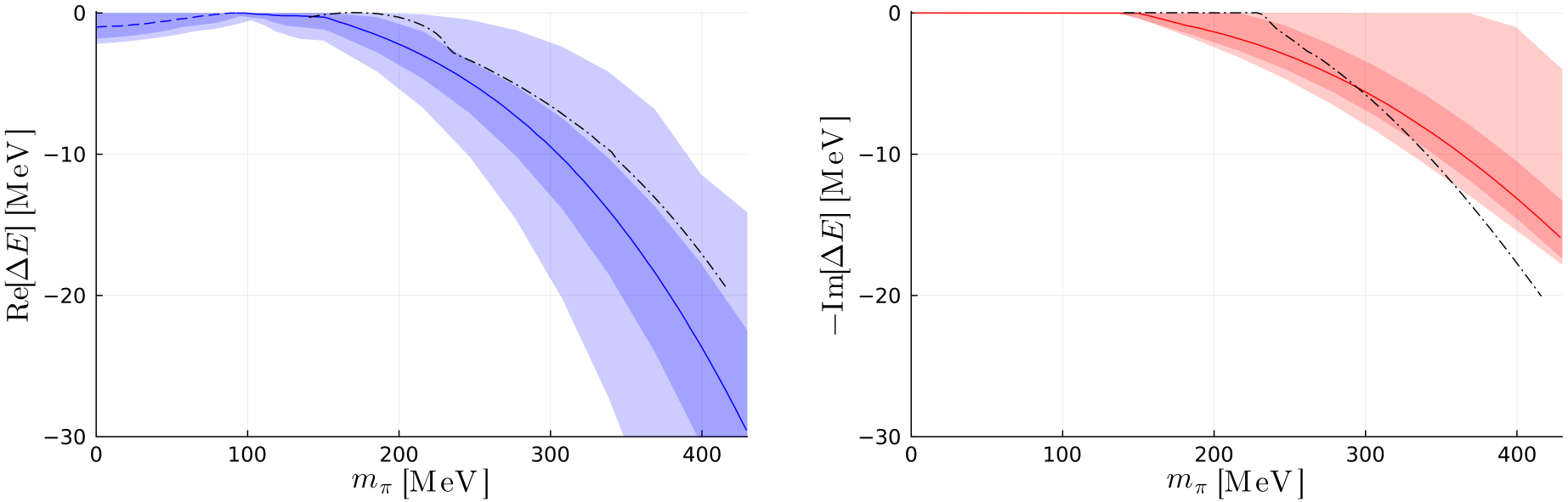

Figure: Dependence of the real and imaginary parts of the pole with the pion mass for the physical charm quark mass trajectory. The dash-dotted black line corresponds to the result of Abolnikov2024.

See also M.L. Du, Baru, Dong, F.K. Guo, et al, PRD22, M.L. Du, Filin, Baru, F.K. Guo et al., PRL23; Meng, Baru et al., PRD24

The $\Lambda(1405)$

Two pole structure

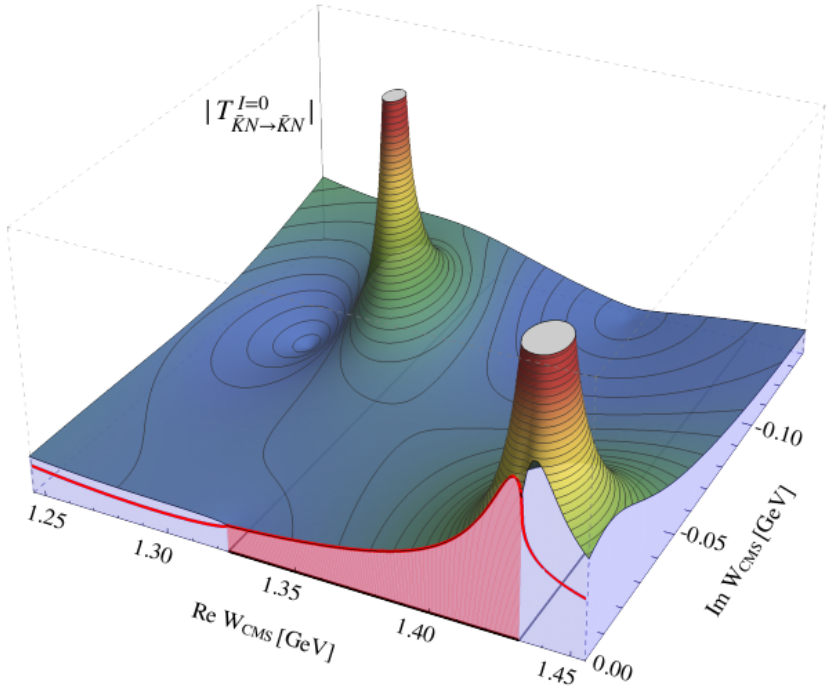

Figure taken from Review of the $\Lambda(1405)$, Mai (2020)

$\pi\Sigma$, $\bar{K}N$

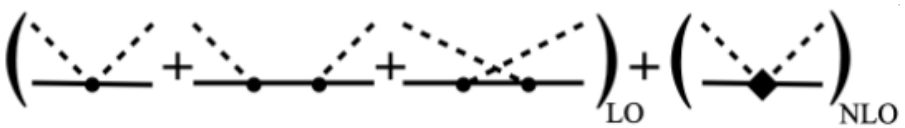

2nd Riemann Sheet

$$\frac{1}{\sqrt{s} - M_R + i\Gamma/2}$$

$$\Gamma/2 = \beta p$$
$$\sqrt{s} = a + ib$$

$$\frac{1}{a - M_R + ib + i\beta p}$$

Change $p \to -p$
gives a solution

Two pole structures

- At LO the interaction is diagonal $V_{\alpha\beta} = -\frac{1}{4f^2} C_{\alpha\beta}(k^0 + k'^0)$.

$$V_{\alpha\beta} = \text{diag}(6, 3, 3, 0, 0, -2) \quad \alpha, \beta = 1, 8, 8', 10, \bar{10}, 27 \qquad (16)$$

- At NLO the accidental symmetry of the two octects is slightly broken ($\Delta M_8 \simeq 15$ MeV) Guo, Kamiya, Mai, Meissner PLB23
- The most important features obtained at LO remain at NNLO.
  (L0) Jido, Oller, Oset, Ramos, Meissner NPA03
  (NNLO) Lu, Geng, Doering, Mai PRL23

$$(LO) \qquad \sqrt{s_0} : 1390 - i\,66, \quad 1426 - i\,16$$
$$(NNLO) \quad \sqrt{s_0} : 1392 \pm 8 - i\,(100 \pm 15),\ 1425 \pm 1 - i\,(13 \pm 4)$$

Weinberg-Tomozawa dominates

BaSc, PRL132 (2024)

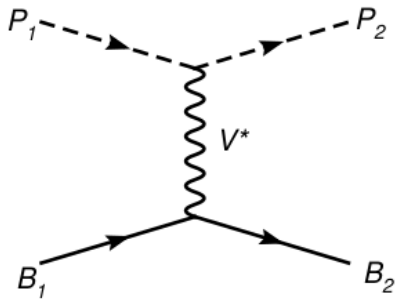

The Chiral Unitary Approach for Meson-Baryon

- Chiral Lagrangians for the Meson-Baryon interaction:
  Pich, RPP95; Ecker, PPNP94, Bernard, Kaisser, Meissner, IJNPE95;
  Meissner, RPP93

$$\mathcal{L} = \mathcal{L}_{\phi} + \mathcal{L}_{\phi B} \,, \tag{17}$$

Lowest order:

$$\mathcal{L}^{(1)}_{\phi B} = i\langle \bar{B}\gamma_\mu [D^\mu, B]\rangle - M_0\langle \bar{B}B\rangle - \frac{1}{2} D\langle \bar{B}\gamma_\mu\gamma_5 \{u^\mu, B\}\rangle - \frac{1}{2} F\langle \bar{B}\gamma_\mu\gamma_5 [u^\mu, B]\rangle$$

Next-to-leading order

$$\begin{aligned}\mathcal{L}^{(2)}_{\phi B} \;=\; & b_D\langle \bar{B}\{\chi_+, B\}\rangle + b_F\langle \bar{B}[\chi_+, B]\rangle + b_0\langle \bar{B}B\rangle\langle \chi_+\rangle \\ & + d_1\langle \bar{B}\{u_\mu, [u^\mu, B]\}\rangle + d_2\langle \bar{B}[u_\mu, [u^\mu, B]]\rangle \\ & + d_3\langle \bar{B}u_\mu\rangle\langle u^\mu B\rangle + d_4\langle \bar{B}B\rangle\langle u^\mu u_\mu\rangle \,,\end{aligned} \tag{18}$$

Chiral Unitary Approach for Meson-baryon

U enters in the combinations $u_\mu = iu^\dagger \partial_\mu U u^\dagger$:

$$U(\phi) = u^2(\phi) = \exp\left(\sqrt{2} i \frac{\phi}{f}\right), \tag{19}$$

Pseudoscalar meson octet ϕ :

$$\phi = \begin{pmatrix} \frac{1}{\sqrt{2}}\pi^0 + \frac{1}{\sqrt{6}}\eta & \pi^+ & K^+ \\ \pi^- & -\frac{1}{\sqrt{2}}\pi^0 + \frac{1}{\sqrt{6}}\eta & K^0 \\ K^- & \bar{K}^0 & -\frac{2}{\sqrt{6}}\eta \end{pmatrix}, \tag{20}$$

The octet baryon fields:

$$B = \begin{pmatrix} \frac{1}{\sqrt{2}}\Sigma^0 + \frac{1}{\sqrt{6}}\Lambda & \Sigma^+ & p \\ \Sigma^- & -\frac{1}{\sqrt{2}}\Sigma^0 + \frac{1}{\sqrt{6}}\Lambda & n \\ \Xi^- & \Xi^0 & -\frac{2}{\sqrt{6}}\Lambda \end{pmatrix}, \tag{21}$$

and the covariant derivative

$$[D_\mu, B] = \partial_\mu B + [\Gamma_\mu, B], \quad \Gamma_\mu = \frac{1}{2}[u^\dagger, \partial_\mu u]. \tag{22}$$

Chiral Unitary Approach for Meson-baryon

Channels for $I = 0, S = -1$: $\pi\Sigma, \bar{K}N, \eta\Lambda, K\Xi$

- Weinberg-Tomozawa+Born+NLO: $\boxed{V_{ij} = V_{ij}^{\rm LO} + V_{ij}^{\rm NLO}}$

where $V^{\rm LO} = V^{\rm WT} + V^{\rm Born}$. WT and NLO terms (Feijoo2015),

$$V_{ij}^{\rm WT} = -\frac{N_i N_j}{4f^2}\left[C_{ij}(2\sqrt{s} - M_i - M_j)\right], \tag{23}$$

$$V_{ij}^{\rm NLO} = -\frac{N_i N_j}{f^2}(D_{ij} - 2k_\mu k'^\mu L_{ij}), \tag{24}$$

$N_i = \sqrt{(M_i + E_i)/2M_i}$. M_i, E_i baryon mass and energy of the channel i

Born, direct s and crossed u (Khemchandani, Martinez-Torres,Oller, 2019)

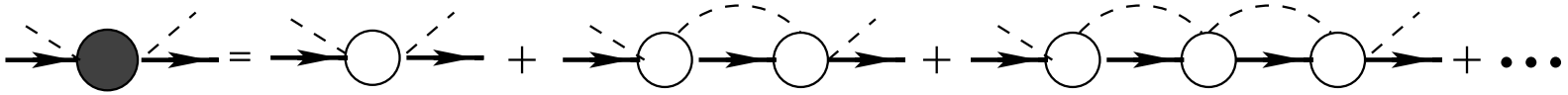

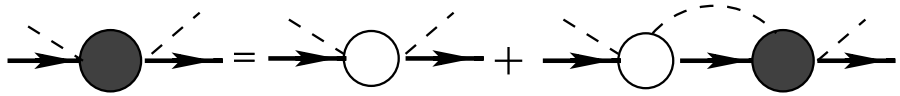

Interaction $I = 0$

Channel basis - SU(3) basis

$$\begin{bmatrix} |\pi\Sigma\rangle \\ |\bar{K}N\rangle \\ |\eta\Lambda\rangle \\ |K\Xi\rangle \end{bmatrix} = \begin{bmatrix} \frac{\sqrt{\frac{3}{2}}}{2} & -\sqrt{\frac{3}{5}} & 0 & -\frac{1}{2\sqrt{10}} \\ -\frac{1}{2} & -\frac{1}{\sqrt{10}} & \frac{1}{\sqrt{2}} & -\frac{\sqrt{\frac{3}{5}}}{2} \\ -\frac{1}{2\sqrt{2}} & -\frac{1}{\sqrt{5}} & 0 & \frac{3\sqrt{\frac{3}{10}}}{2} \\ \frac{1}{2} & \frac{1}{\sqrt{10}} & \frac{1}{\sqrt{2}} & \frac{\sqrt{\frac{3}{5}}}{2} \end{bmatrix} \begin{bmatrix} |1\rangle \\ |8\rangle \\ |8'\rangle \\ |27\rangle \end{bmatrix}$$

SU(3) limit LO+WT+Born s, u channels+NLO

$$C_{\mathrm{SU}(3)}^{\mathrm{WT}} = \begin{bmatrix} 6 & & & \\ & 3 & & \\ & & 3 & \\ & & & -2 \end{bmatrix}$$

$$C_{\mathrm{SU}(3)}^{\mathrm{Born}-s} = \begin{bmatrix} 0 & 0 & 0 & 0 \\ 0 & \frac{10D^2}{3} & -2\sqrt{5}DF & 0 \\ 0 & -2\sqrt{5}DF & 3F^2 & 0 \\ 0 & 0 & 0 & 0 \end{bmatrix}, \quad C_{\mathrm{SU}(3)}^{\mathrm{Born}-u} = \begin{bmatrix} \frac{10D^2}{3} - 6F^2 & 0 & 0 & 0 \\ 0 & -D^2 - 3F^2 & 0 & 0 \\ 0 & 0 & 3F^2 - \frac{5D^2}{3} & 0 \\ 0 & 0 & 0 & \frac{2}{3}(D^2 + 3F^2) \end{bmatrix},$$

$$C_{\mathrm{SU}(3)}^{\mathrm{NLO1}} = \begin{bmatrix} \frac{4}{3}m^2(3b_0 + 7b_D) & 0 & 0 & 0 \\ 0 & \frac{2}{3}m^2(6b_0 + b_D) & -2\sqrt{5}m^2 b_F & 0 \\ 0 & -2\sqrt{5}m^2 b_F & 2m^2(2b_0 + 3b_D) & 0 \\ 0 & 0 & 0 & 4m^2(b_0 + b_D) \end{bmatrix},$$

$$C_{\mathrm{SU}(3)}^{\mathrm{NLO2}} = \begin{bmatrix} -6d_2 + 9d_3 + 2d_4 & 0 & 0 & 0 \\ 0 & -3d_2 + d_3 + 2d_4 & -\sqrt{5}d_1 & 0 \\ 0 & -\sqrt{5}d_1 & 9d_2 - d_3 + 2d_4 & 0 \\ 0 & 0 & 0 & 2d_2 + d_3 + 2d_4 \end{bmatrix},$$

Covariant baryon chiral perturbation

- Input: RQCD, JHEP23. Chiral trajectories $\mathrm{Tr}[M] = \mathrm{C}$, $m_s = m_{s,\mathrm{phy}}$, and $m_s = m_l$, $l = u, d$
- CoBChPT. J. Martín-Camalich, L. S. Geng. M. J. Vicente-Vacas, JHEP05(2023)

$$m_B = m_0 + m_B^{(2)} + m_B^{(3)} \ , \tag{25}$$

$$m_B^{(2)} = \sum_{\phi=\pi,K} -\xi_{B,\phi}^{(a)} m_\phi^2, \tag{26}$$

$$m_B^{(3)} = \sum_{\phi=\pi,K,\eta} \frac{1}{(4\pi f_\phi)^2} \xi_{B,\phi}^{(b)} H_B^{(b)}(m_\phi) \ , \tag{27}$$

Polinomial+loop. D, F (nuclear beta decay, Borasoy, PRD98)

$$D = 0.80, \ F = 0.46. \tag{28}$$

Covariant baryon chiral perturbation

	m_0 [MeV]	b_0 [GeV^{-1}]	b_D [GeV^{-1}]	b_F [GeV^{-1}]
This work	805(40)(40)	−0.665(40)(28)	0.062(26)(8)	−0.354(18)(9)
RQCD23	$821^{(71)}_{(53)}$	$-0.739^{(70)}_{(84)}$	$0.056^{(43)}_{(39)}$	$-0.44^{(40)}_{(26)}$

- Covariance matrix obtained in the LQCD simulation is taken into account

$$\chi^2 = \Delta E^T C_E^{-1} \Delta E \tag{29}$$

b_i are related to the splitting of the octect baryon masses and pion-nucleon sigma term (Gasser,PLB91). Chiral trajectories:

$$m_{0K}^2 = B_0 C - \frac{m_{0\pi}^2}{2}, \quad \mathrm{Tr}[M] = \mathrm{C}$$

$$m_{0K}^2 = B_0 m_{s,\mathrm{ph}} + \frac{m_{0\pi}^2}{2}, \quad m_s = m_{s,\mathrm{ph}} \tag{30}$$

Covariant baryon chiral perturbation

Figure: Baryon masses over the different chiral trajectories.

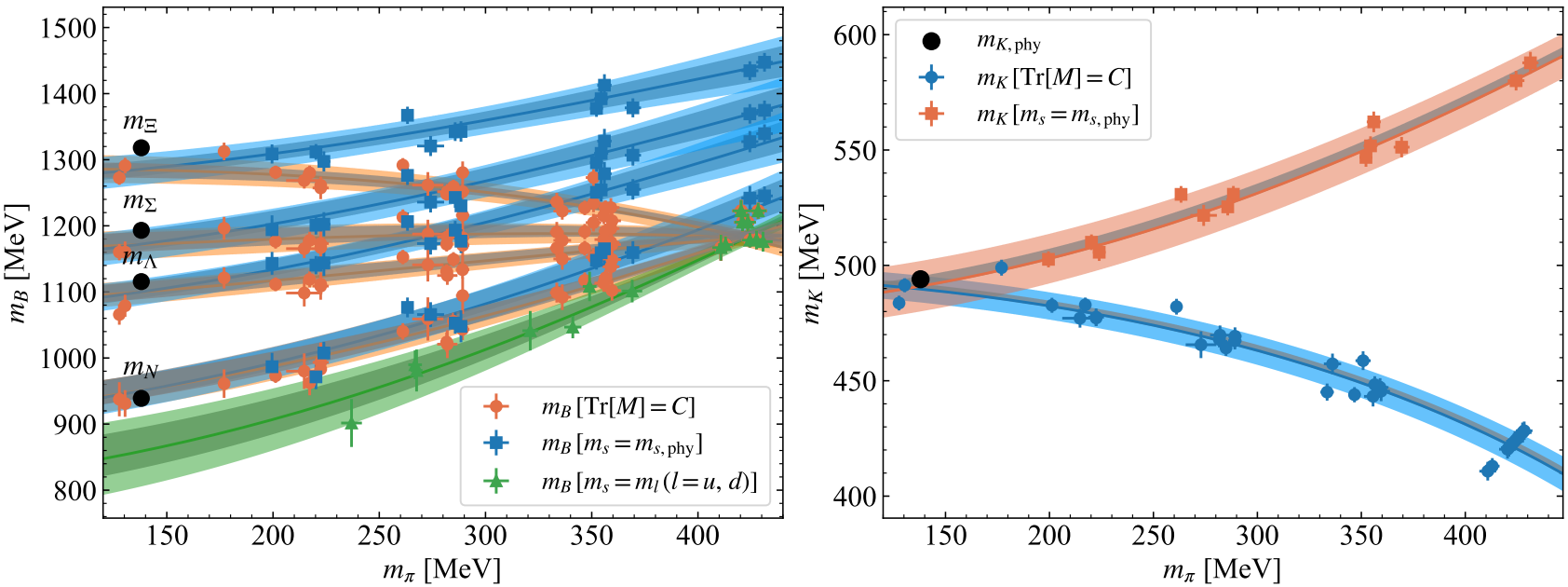

For the masses and decay constants of pseudoscalar mesons, we take the LECs L_i^r's from a global fit that includes also the data of the CLS ensembles, Molina and Ruiz de Elvira, JHEP20

Energy Levels for $\bar{K}N - \pi\Sigma$ scattering ($I = 0$)

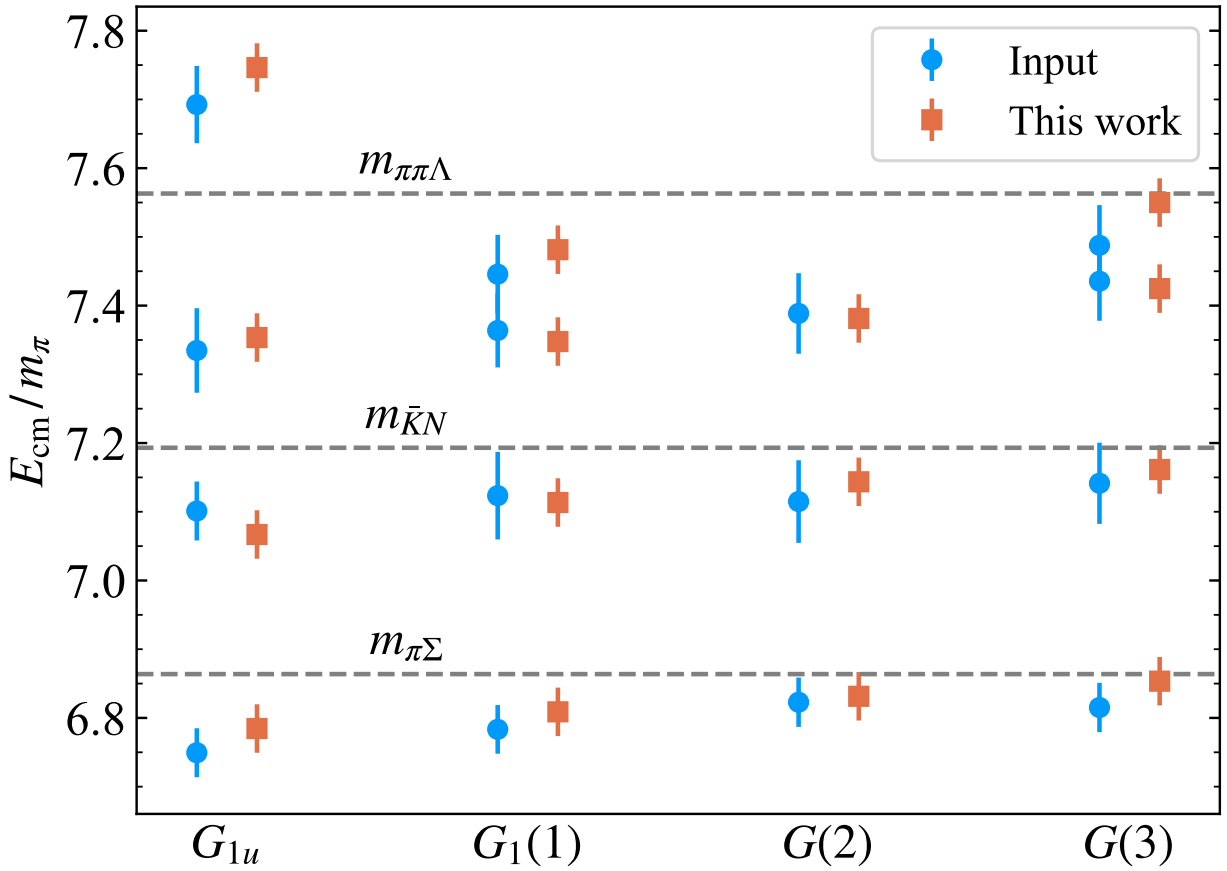

Figure: Finite-volume spectrum (circle points) in the center-of-mass frame used as input to constrain the free parameters of the chiral Lagrangian up to NLO. Input: J. Bulava, BaSc, PRD24, PRL24.

LECs, cutoff, SC, poles, couplings ...

d_1	d_2	d_3	d_4	$q_{\max}$ [MeV]
−0.38(9)(7)	0.02(1)(1)	−0.07(3)(3)	−0.45(5)(6)	623(23)(23)

Table: Results for the LECs and cutoff $q_{\max}$ obtained in the fit. LECs in GeV^{-1}.

We obtain $a \simeq -2$ (natural value, Oller, Meissner, PLB01).

$$a_{\pi\Sigma} = -2.18,\ a_{\bar{K}N} = -1.89 \quad m_\pi = 138\ \mathrm{MeV}$$

$$a_{\pi\Sigma} = -2.15,\ a_{\bar{K}N} = -1.92 \quad m_\pi = 200\ \mathrm{MeV}$$

$$a_{\bar{K}N} = a_{\pi\Sigma} = -2.08 \quad m_\pi = 423\ \mathrm{MeV}\ (\mathrm{SU3\ limit})$$

The value of $q_{\max}$ is similar to Oset, Ramos, NPA98 (630 MeV).

LECs, cutoff, SC, poles, couplings ..

	m_π (MeV)	Pole (MeV)	$\lvert g_{\pi\Sigma}\rvert$	$\lvert g_{\bar{K}N}\rvert$	$\left\lvert \frac{g_{\pi\Sigma}}{g_{\bar{K}N}} \right\rvert$	$\lvert g_{\eta\Lambda}\rvert$	$\lvert g_{K\Xi}\rvert$
4 channels	138	$1376(10)(10) - i142(19)(5)$	2.8(1)(2)	2.3(6)(3)	1.2(5)(1)	1.5(3)(3)	1.0(1)(2)
		$1418(11)(2) - i11(6)(3)$	1.1(5)(2)	3.0(2)(2)	0.4(1)(1)	2.0(2)(5)	0.4(1)(3)
	200	$1366^{(43)(19)}_{(6)(3)} - i57^{(42)(23)}_{(57)(57)}$	3.7(7)(4)	1.8(8)(6)	2.1(5)(3)	1.2(3)(3)	0.8(2)(2)
		$1450(15)(11) - i15(9)(5)$	1.5(7)(4)	3.1(5)(4)	0.5(2)(1)	2.1(3)(6)	0.5(1)(3)
2 channels	200	1387(7)(6)	3.4(10)(10)	1.8(5)(8)	1.9(10)(5)	...	...
		$1455(14)(6) - i29(11)(7)$	2.2(7)(3)	3.8(6)(3)	0.6(1)(1)	...	...

TABLE III. Pole positions and couplings of the $\Lambda(1405)$ for $m_\pi = 138$ and 200 MeV.

Pole positions and couplings in LQCD ($m_\pi \simeq 200$ MeV):
$z_1 = 1392(9)(2)(16)$ MeV, $z_2 = 1455(13)(2)(17) - i11.5(4.4)(4)(0.1)$
Ratios of the couplings:

$$\left|\frac{g^{(1)}_{\pi\Sigma}}{g^{(1)}_{\bar{K}N}}\right| = 1.9(4)_{\rm st}(6)_{\rm md}, \quad \left|\frac{g^{(2)}_{\pi\Sigma}}{g^{(2)}_{\bar{K}N}}\right| = 0.53(9)_{\rm st}(10)_{\rm md},$$

LECs, cutoff, SC, poles, couplings ...

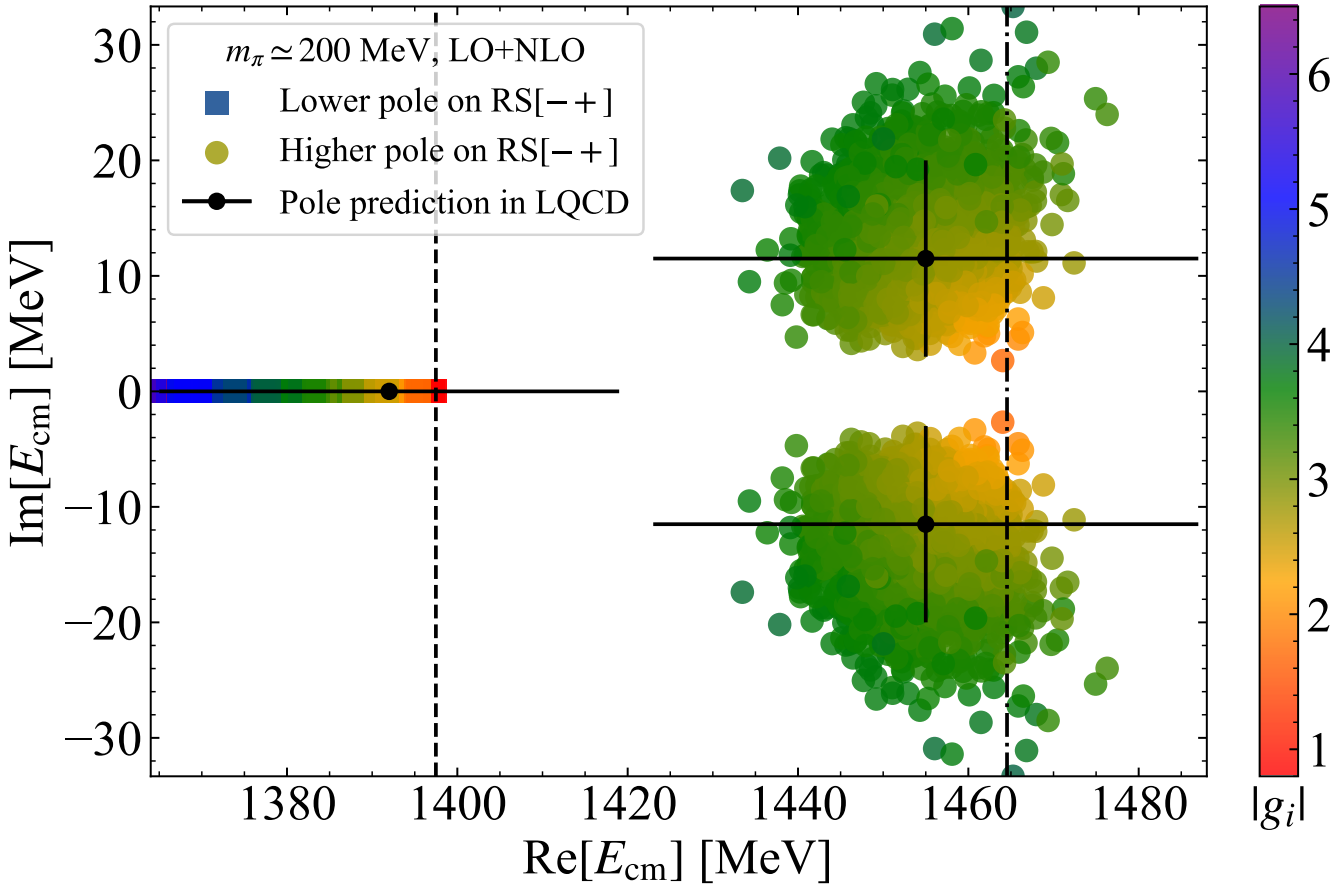

Figure: Pole positions of the $\Lambda(1405)$ for $m_\pi \simeq 200$ MeV at 1-σ(68%) confidence level. The error bars in black denote the LQCD results. The dashed line represents the $\pi\Sigma$ threshold and the dot-dashed line is the $\bar{K}N$ threshold.

Phase shifts up to NLO

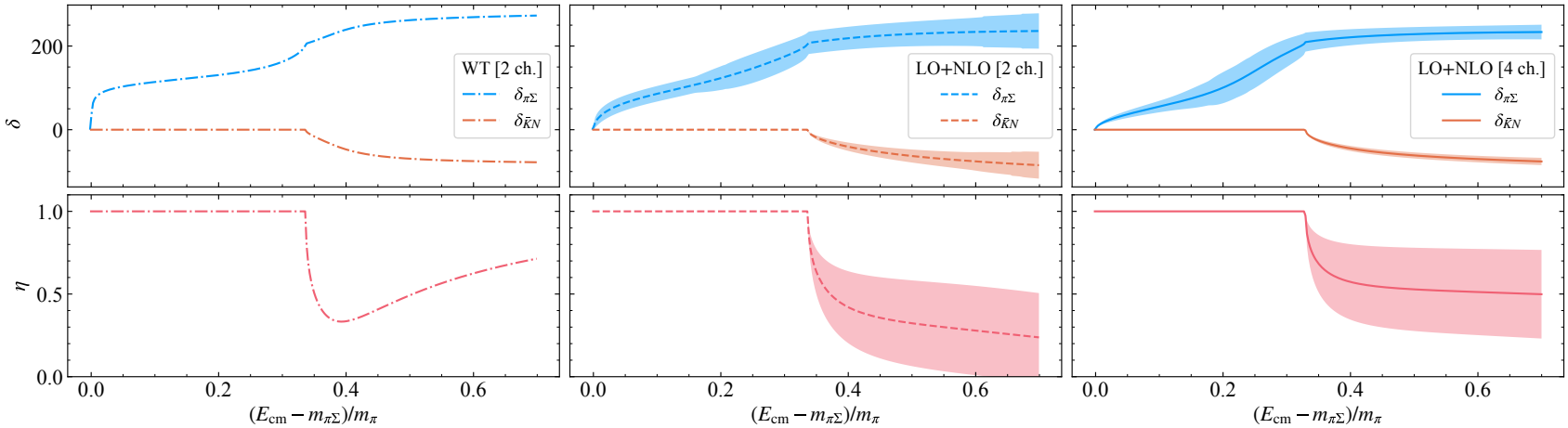

(LQCD, BaSc, PRD24, PRL24)

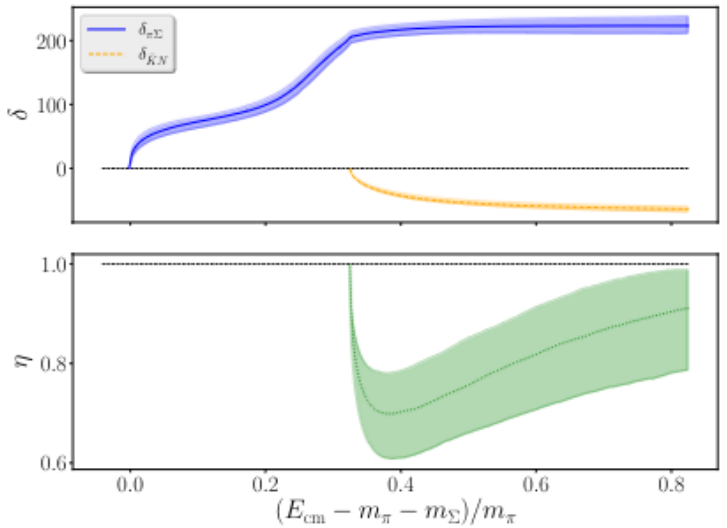

Comparison with experiment

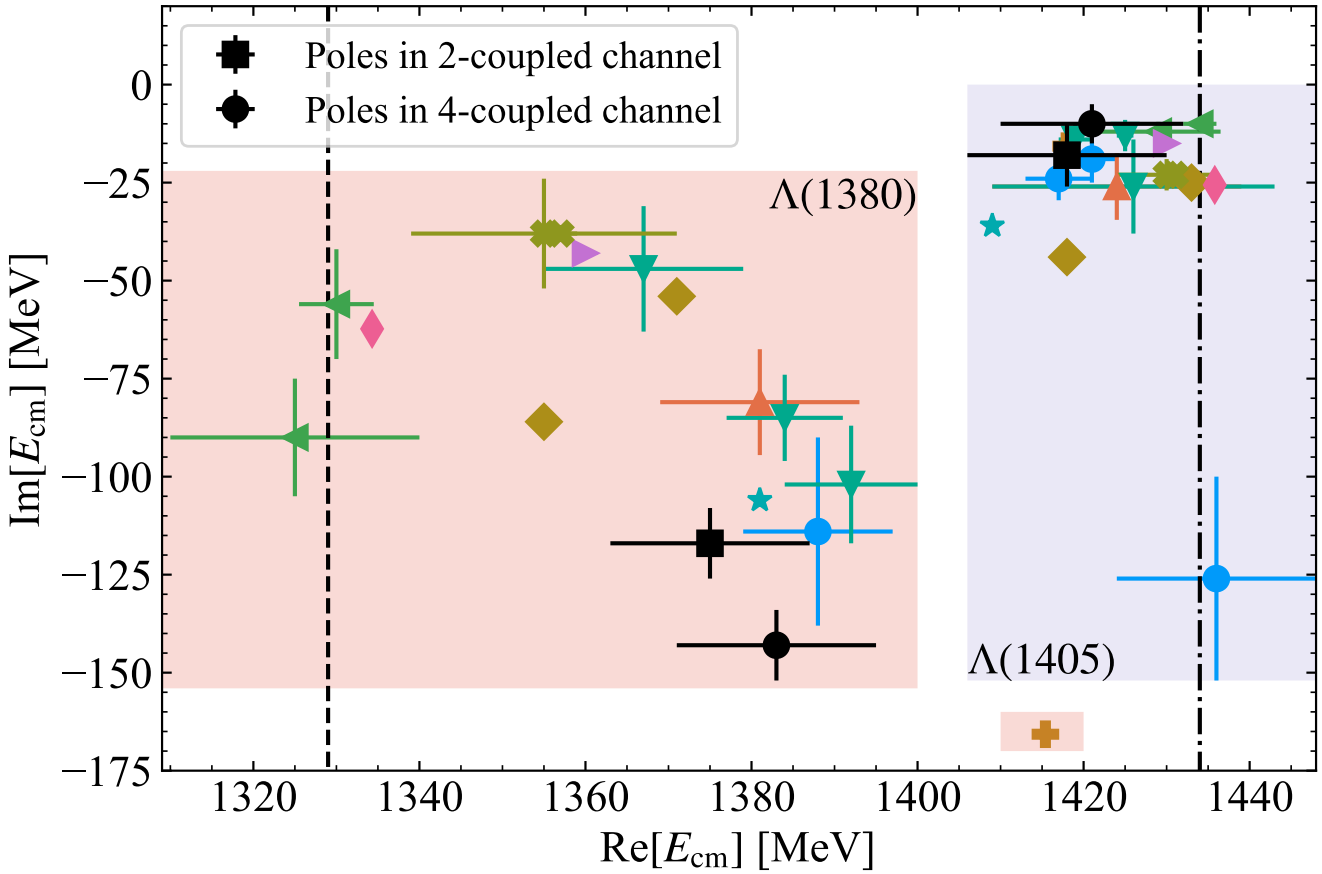

NLO: Guo12 Ikeda12 Mai14 Sadasivan2018 Cieply11 Shevchenko11 Haidenbauer10 Guo23 Sadasivan:22
NNLO: Lu22

Figure: Pole positions of the two $\Lambda(1405)$ in comparison with other studies.

Comparison with experiment

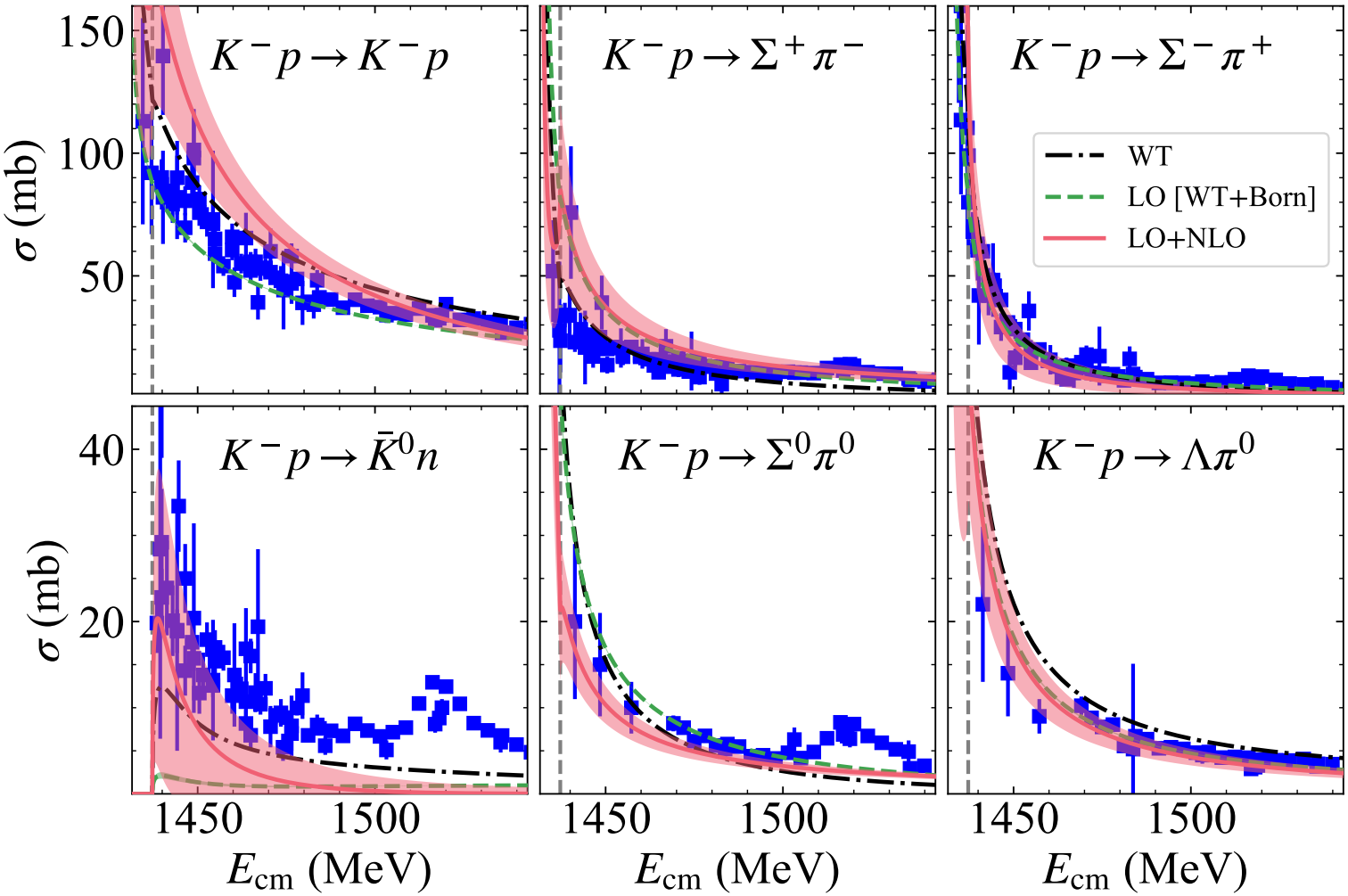

Figure: Comparison of the cross sections predicted by the model and the experimental data.

SU(3) limit

We define:

$$|8_a> = \cos\theta|8> - \sin\theta|8'>,$$
$$|8_b> = \cos\theta|8> + \sin\theta|8'>, \qquad (31)$$

$$I = 0; \quad a_{\bar{K}N} = a_{\pi\Sigma} = -2.08; \quad m_\pi = 423 \text{ MeV}; \quad \theta \simeq -60^o$$

	WT			LO [WT+Born]			LO+NLO		
	z_1	z_2	z_3	z_1	z_2	z_3	z_1	z_2	z_3
Pole (MeV)	1556(2)	1606(1)	1606(1)	1548(3)	1601(1)	1607(1)	1573(6)(6)	1589(7)(5)	1603(9)(10)
$\lvert g_{(1)}\rvert$	3.0(1)	0	0	3.0(1)	0	0	2.8(1)(1)	0	0
$\lvert g_{(8_a)}\rvert$	0	0.8(1)	0	0	1.8(1)	0	0	2.4(8)(2)	0
$\lvert g_{(8_b)}\rvert$	0	0	0.8(1)	0	0	0.4(1)	0	0	1.7(6)(5)

TABLE IV. Pole positions and couplings to the relevant multiplets in the SU(3) limit.

Up to NLO, i.e., $\Delta E^{(8)} = E^{(8_b)} - E^{(8_a)} = 14$ MeV. More than 140 MeV difference with Guo, Kamiya, Mai, Meissner PLB23: 1704 and 1788 MeV, $\Delta E_8 = 15$ MeV

Trajectories of the poles towards SU(3)

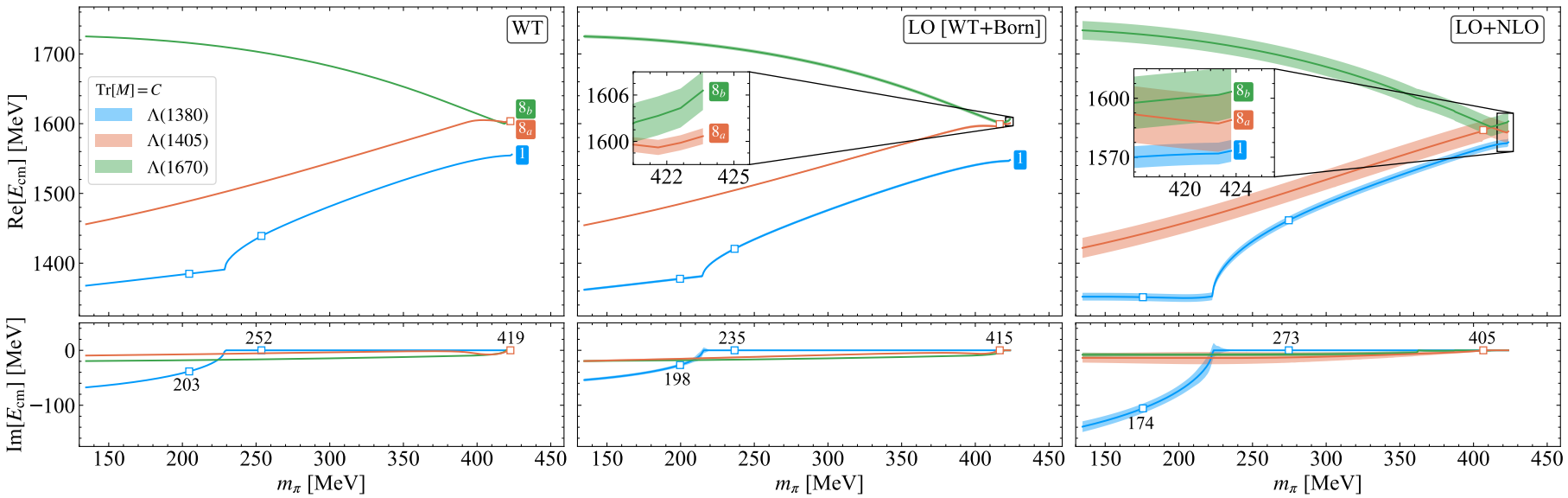

Figure: Trajectories of the three poles up to NLO for the $\Lambda(1405)$ and $\Lambda(1670)$ along the curve $\mathrm{Tr}[M] = C$.

We do not observe that the trajectories exchange when the NLO is included (Guo, Kamiya, Mai, Meissner PLB23). Result in qualitative agreement with Jido, Oset, Ramos, Meissner, NPA03, and Bruns, Cieply, NPA22.

Trajectories of the poles towards SU(3)

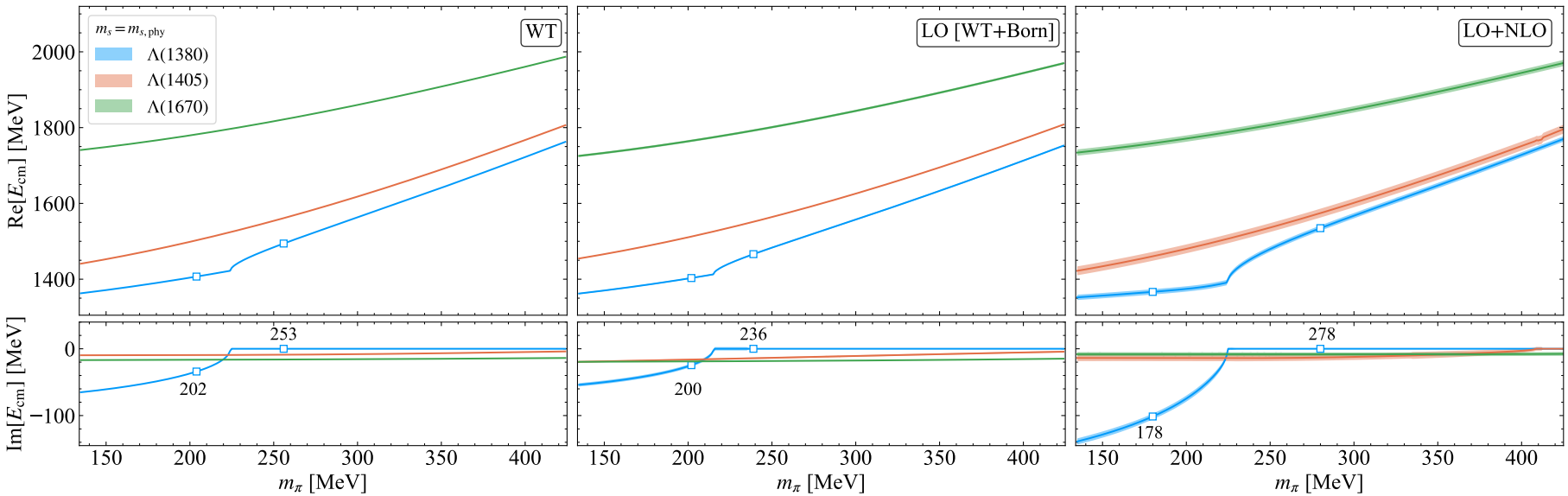

Figure: Trajectories of the three poles up to NLO for the $\Lambda(1405)$ and $\Lambda(1670)$ along the curve $m_s = m_{s,\mathrm{phy}}$.

Prediction for $I = 1$

Ch. basis - SU(3) basis

SU(3) limit, LO+WT+Born s, u channels

$$\begin{bmatrix} |\pi\Lambda\rangle \\ |\pi\Sigma\rangle \\ |\bar{K}N\rangle \\ |\eta\Sigma\rangle \\ |K\Xi\rangle \end{bmatrix} = \begin{bmatrix} \frac{1}{\sqrt{5}} & 0 & \frac{1}{2} & \frac{1}{2} & \sqrt{\frac{3}{10}} \\ 0 & \sqrt{\frac{2}{3}} & \frac{1}{\sqrt{6}} & -\frac{1}{\sqrt{6}} & 0 \\ -\sqrt{\frac{3}{10}} & -\frac{1}{\sqrt{6}} & \frac{1}{\sqrt{6}} & -\frac{1}{\sqrt{6}} & \frac{1}{\sqrt{5}} \\ \frac{1}{\sqrt{5}} & 0 & -\frac{1}{2} & -\frac{1}{2} & \sqrt{\frac{3}{10}} \\ -\sqrt{\frac{3}{10}} & \frac{1}{\sqrt{6}} & -\frac{1}{\sqrt{6}} & \frac{1}{\sqrt{6}} & \frac{1}{\sqrt{5}} \end{bmatrix} \begin{bmatrix} |8\rangle \\ |8'\rangle \\ |10\rangle \\ |\bar{10}\rangle \\ |27\rangle \end{bmatrix}$$

$$C_{\mathrm{SU}(3)}^{\mathrm{WT}} = \begin{bmatrix} 3 & 0 & 0 & 0 & 0 \\ 0 & 3 & 0 & 0 & 0 \\ 0 & 0 & 0 & 0 & 0 \\ 0 & 0 & 0 & 0 & 0 \\ 0 & 0 & 0 & 0 & -2 \end{bmatrix}$$

$$C_{\mathrm{SU}(3)}^{\mathrm{Born}-s} = \begin{bmatrix} \frac{10}{3}D^2 & -2\sqrt{5}DF & 0 & 0 & 0 \\ -2\sqrt{5}DF & 6F^2 & 0 & 0 & 0 \\ 0 & 0 & 0 & 0 & 0 \\ 0 & 0 & 0 & 0 & 0 \\ 0 & 0 & 0 & 0 & 0 \end{bmatrix}, \quad C_{\mathrm{SU}(3)}^{\mathrm{Born}-u} = \begin{bmatrix} -D^2-3F^2 & 0 & 0 & 0 & 0 \\ 0 & 3F^2-\frac{5D^2}{3} & 0 & 0 & 0 \\ 0 & 0 & \frac{4}{3}D(D+3F) & 0 & 0 \\ 0 & 0 & 0 & \frac{4}{3}D(D-3F) & 0 \\ 0 & 0 & 0 & 0 & \frac{2}{3}(D^2+3F^2) \end{bmatrix},$$

$$C_{\mathrm{SU}(3)}^{\mathrm{NLO1}} = \begin{bmatrix} \frac{2}{3}m^2(6b_0+b_D) & -2\sqrt{5}m^2b_F & 0 & 0 & 0 \\ -2\sqrt{5}m^2b_F & 2m^2(2b_0+3b_D) & 0 & 0 & 0 \\ 0 & 0 & 4m^2(b_0+b_F) & 0 & 0 \\ 0 & 0 & 0 & 4m^2(b_0-b_F) & 0 \\ 0 & 0 & 0 & 0 & 4m^2(b_0+b_D) \end{bmatrix},$$

$$C_{\mathrm{SU}(3)}^{\mathrm{NLO2}} = \begin{bmatrix} -3d_2+d_3+2d_4 & -\sqrt{5}d_1 & 0 & 0 & 0 \\ -\sqrt{5}d_1 & 9d_2-d_3+2d_4 & 0 & 0 & 0 \\ 0 & 0 & 2d_1-d_3+2d_4 & 0 & 0 \\ 0 & 0 & 0 & -2d_1-d_3+2d_4 & 0 \\ 0 & 0 & 0 & 0 & 2d_2+d_3+2d_4 \end{bmatrix}.$$

Prediction for $I = 1$

$m_\pi = 138$ MeV

TABLE V. Pole positions and couplings of the two $I = 1$ states at the physical point.

Pole (MeV)	$\lvert g_{\pi\Lambda}\rvert$	$\lvert g_{\pi\Sigma}\rvert$	$\lvert g_{\bar{K}N}\rvert$	$\lvert g_{\eta\Sigma}\rvert$	$\lvert g_{K\Xi}\rvert$
$1345^{(63)}_{(15)} - i315^{(16)}_{(18)}$	0.3(1)	2.2(2)	2.3(2)	0.8(4)	1.6(1)
$1447^{(25)}_{(47)} - i4^{(20)}_{(4)}$	0.9(1)	1.2(2)	2.5(2)	1.6(4)	0.3(1)

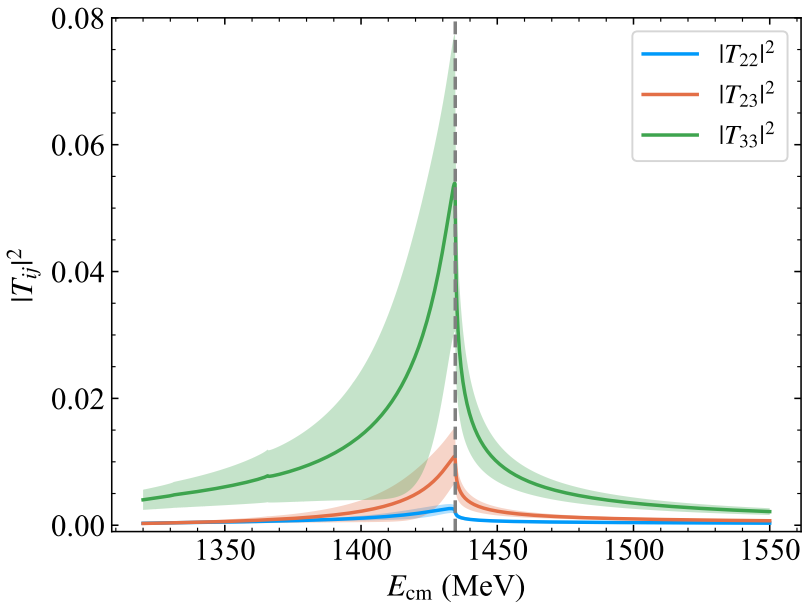

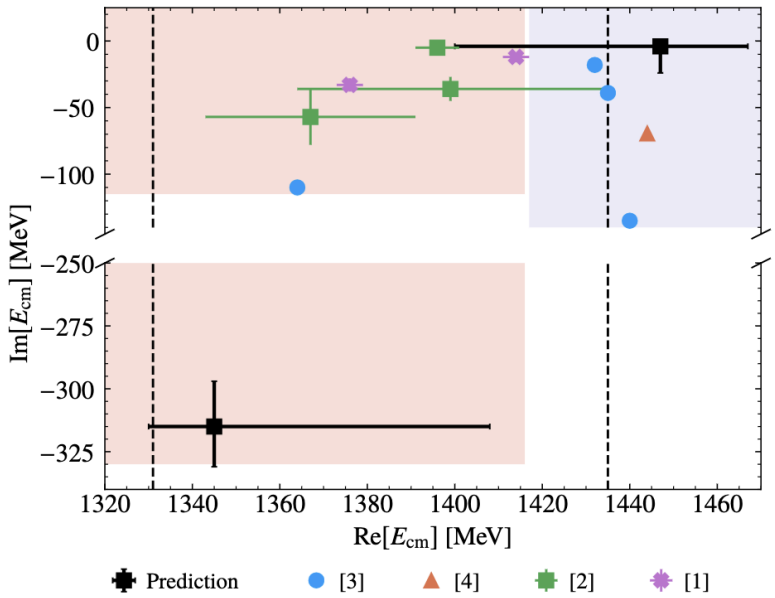

[1] Z.-H. Guo et al, PRC, 87, 035202 (2013) [2] K. P. et al, PRC, 100, 015208 (2019)

[3] J.-X. Lu et al, PRL, 130, 071902 (2023) [4] J. A. Oller et al, PLB, 500:263-272 (2001)

Prediction for $I = 1$, $m_\pi = 423$ MeV

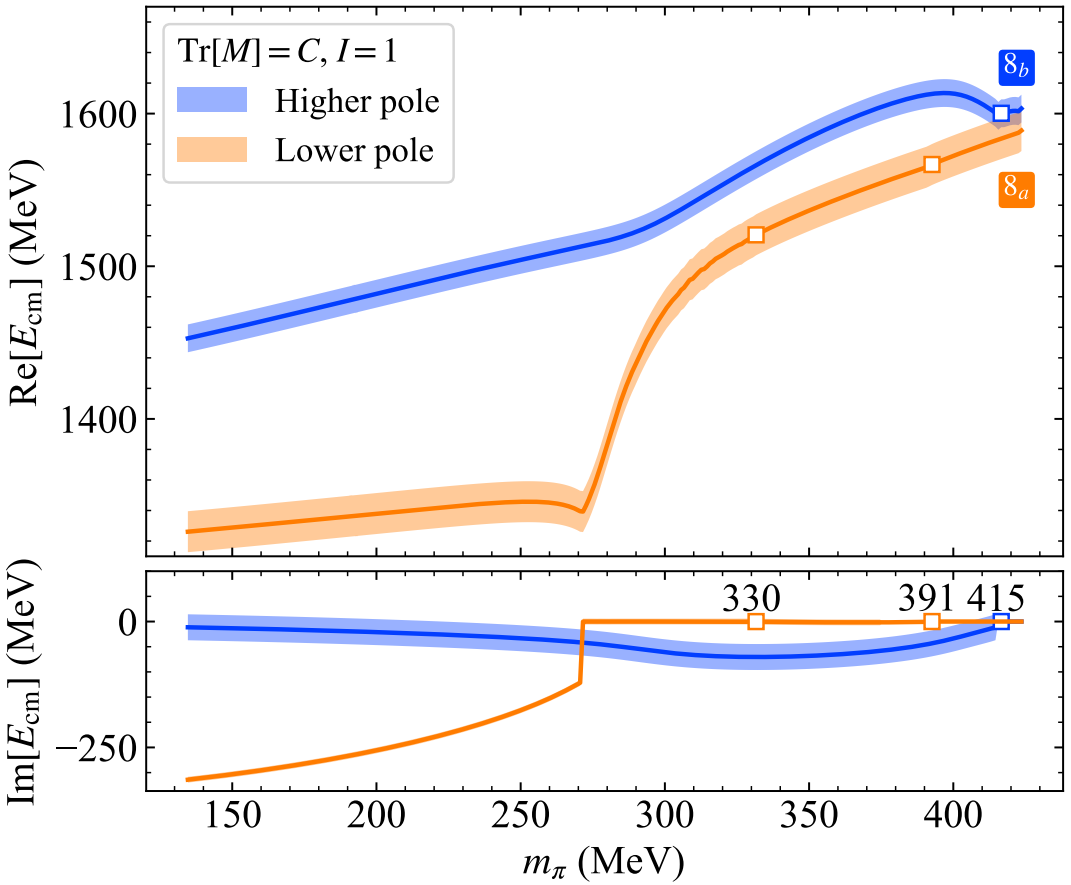

SU(3) limit: 2 bound states, $E_{(8_a)} = 1589(8)$ MeV, $E_{(8_b)} = 1603(9)$ MeV

Conclusions

- The combination of finite volume-EFT with LQCD is an useful tool to study the quark mass dependence of resonances
- Our study also supports the molecular interpretation of the T_{cc} as generated by the DD^* interaction
- The results of the LQCD simulation for the T_{cc} are compatible with a virtual state that is transitioning into a bound state for a pion mass close to physical and with the vector meson exchange being dominant, Gil-Dominguez, Giachino and Molina, PRD25
- We have conducted a precise study for the $\Lambda(1405)$ quark mass dependence and the two-pole trajectories to the SU(3) limit that supports the two-pole structure
- We find also that this LQCD data analysis is consistent with experimental data and we made predictions for $I = 1$ Z. Zhuang, Molina, Junxu-Lu, L. S. Geng, SciBull25